

**Nonlinear Oscillations Under
Multifrequency Parametric Excitation**

by

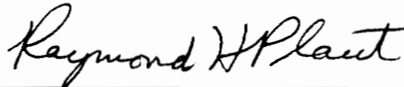
Jeanette J. Gentry

Thesis submitted to the Faculty of the
Virginia Polytechnic Institute and State University
in partial fulfillment of the requirements for the degree of
Master of Science
in
Engineering Mechanics

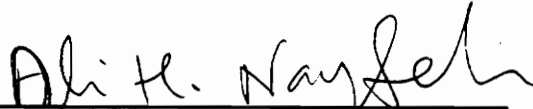
APPROVED:



Dr. Dean T. Mook, Co-Chairman



Dr. Raymond H. Plaut, Co-Chairman



Dr. Ali H. Nayfeh

November, 1988

Blacksburg, Virginia

2

LD
5655
V855
1988
G467
C.2

000000

**Nonlinear Oscillations Under
Multifrequency Parametric Excitation**

by

Jeanette J. Gentry

Dr. Dean T. Mook, Co-Chairman

Dr. Raymond H. Plaut, Co-Chairman

Engineering Mechanics

(ABSTRACT)

191/121
797

A second-order system of differential equations containing a multifrequency parametric excitation and weak quadratic and cubic nonlinearities is investigated. The method of multiple scales is used to carry out a general analysis, and three resonance conditions are considered in detail. First, the case in which the sum of two excitation frequencies is near two times a natural frequency, $\lambda_s + \lambda_t \simeq 2\omega_q$, is examined. Second, the influence of an internal resonance, $\omega_q \simeq 3\omega_r$, on the previous case is studied. Finally, the effect of the internal resonance $\omega_r \simeq 3\omega_q$ on the resonance $\lambda_s + \lambda_t \simeq 2\omega_q$ is investigated. Results are presented as plots of response amplitudes as functions of a detuning parameter, excitation amplitude, and, for the first case, a measure of the relative values of λ_s and λ_t .

When the parametric resonance, $\lambda_s + \lambda_t \simeq 2\omega_q$, is the only resonance present, no more than one stable nontrivial solution is possible for the parameters studied. Addition of the internal resonance, $\omega_q \simeq 3\omega_r$, to the parametric resonance produces at most one new stable nontrivial solution. Therefore, including the stable nontrivial solutions from the parametric resonance only, up to three stable steady-state solutions are present for certain parameter ranges. The internal resonance, $\omega_r \simeq 3\omega_q$, eliminates the solutions for $\lambda_s + \lambda_t \simeq 2\omega_q$ only, and again no more than one stable

nontrivial solution is present for any given set of parameters. In this case, there are regions where no stable solutions are possible.

Acknowledgements

I would like to thank Dr. Plaut and Dr. Mook for their guidance, support, and most of all, their patience throughout my efforts on this thesis. Special thanks are extended to Sally Schrader whose good humor and knowledge of GML have been invaluable. I would also like to express my appreciation to my family and friends for their love and encouragement. Finally, I would like to thank the U. S. Army Research Office for supporting this work.

Table of Contents

Chapter 1.	
Introduction	1
Literature Review	3
Chapter 2. Analysis	7
Chapter 3. The Case When $\lambda_s + \lambda_t \simeq 2\omega_q$	13
Chapter 4. The Case When $\lambda_s + \lambda_t \simeq 2\omega_q$ and $\omega_q \simeq 3\omega_r$	29
Chapter 5. The Case When $\lambda_s + \lambda_t \simeq 2\omega_q$ and $3\omega_q \simeq \omega_r$	43
Bibliography.	55
Appendix A. Coefficients and Arguments in Equation (2.20)	57
Vita.	58

List of Illustrations

Figure 1. Frequency-response curves for the case when $\lambda_s + \lambda_t \simeq 2\omega_q$ 25

Figure 2. Response amplitude as a function of excitation amplitude
for the case when $\lambda_s + \lambda_t \simeq 2\omega_q$ 26

Figure 3. Response amplitude as a function of $\lambda_s/(2\omega_q)$ 27

Figure 4. Response amplitude as a function of Q_s when Q_t is fixed 28

Figure 5. Frequency-response curves
for the case when $\lambda_s + \lambda_t \simeq 2\omega_q$ and $\omega_q \simeq 3\omega_r$ 40

Figure 6. Repeat of Figure 5 with unstable solutions removed
and corresponding solutions marked 41

Figure 7. Response amplitudes as functions of excitation amplitude
for the case when $\lambda_s + \lambda_t \simeq 2\omega_q$ and $\omega_q \simeq 3\omega_r$ 42

Figure 8. Frequency-response curves
for the case when $\lambda_s + \lambda_t \simeq 2\omega_q$ and $3\omega_q \simeq \omega_r$ 52

Figure 9. Response amplitudes as functions of excitation amplitude
for the case when $\lambda_s + \lambda_t \simeq 2\omega_q$ and $3\omega_q \simeq \omega_r$ 53

Figure 10. Limit-cycle behavior in a region
where no stable steady-state solutions exist 54

Chapter 1

Introduction

In this thesis the behavior of a multidegree-of-freedom system subjected to a parametric excitation having multiple harmonic components and containing quadratic and cubic nonlinearities is studied. A parametric excitation appears as a time-varying coefficient in the governing equations of motion. Many natural phenomena such as waves, earthquakes, and wind produce forces which may appear as parametric excitations in the equations governing structures on which they act. Rotating machinery and pumps are examples of man-made devices which may produce the same effect. Parametric excitations act on missiles, rotors and fluid-conveying pipes as well as numerous other mechanical and structural systems.

The system of governing equations examined here,

$$\begin{aligned}
& \ddot{u}_n + 2\varepsilon c_n(\varepsilon)\dot{u}_n + \omega_n^2 u_n + 2\varepsilon \sum_{m=1}^M \cos(\lambda_m t + \tau_m) \sum_{j=1}^{\infty} Q_{jn}^m(\varepsilon) u_j \\
& + \varepsilon \sum_{j=1}^{\infty} \sum_{k=1}^{\infty} \Lambda_{jkn} u_j u_k + \varepsilon^2 \sum_{j=1}^{\infty} \sum_{k=1}^{\infty} \sum_{l=1}^{\infty} \Gamma_{jkl n} u_j u_k u_l = 0; \quad n = 1, 2, \dots,
\end{aligned} \tag{1.1}$$

is typical of those encountered when using discretizing methods such as Rayleigh-Ritz or finite elements. Another discretizing method, modal analysis, reduces governing partial differential equations in space and time to ordinary differential equations and often results in an infinite set similar to (1.1).

In (1.1), the u_n are generalized coordinates, the dots denote derivatives with respect to time, the c_n are damping coefficients, and the ω_n are the linear natural frequencies. The Q_{jn}^m , λ_m , and τ_m are the amplitudes, frequencies and phases of the excitation, respectively, and the amplitudes, frequencies, and phases of the excitations are independent. The Λ_{jkn} and $\Gamma_{jkl n}$ are constant coefficients of the nonlinear terms, and ε is a small dimensionless parameter.

Using the method of multiple scales (MMS), we will determine the equations governing the steady-state amplitudes and phases of the response when certain resonance conditions are met. MMS provides a means of obtaining approximate analytical solutions of systems such as (1.1), which are valid for small but finite values of ε . The transient solution of the nonlinear problem does not necessarily decay as it does for the linear case, and we will see that MMS predicts multivalued nontrivial solutions unlike linear approximations.

Literature Review

Attention is focused here on works involving systems whose only excitation is parametric with multiple harmonic components. In many cases, a single frequency cannot satisfactorily describe a dynamic force, and in these situations a multifrequency excitation provides a more accurate model. A general multifrequency excitation can be written in the form

$$\sum_{m=1}^M P_m \cos(\lambda_m t + \phi_m) \quad (1.2)$$

where the P_m , λ_m , and ϕ_m are the amplitudes, frequencies, and phases, respectively. Excitations involving $\cos \lambda t$ and $\sin \lambda t$ can be written in the form of (1.2) by rewriting $\sin \lambda t = \cos(\lambda - \pi/2)$. Similarly, coefficients such as $(a + b \cos \lambda t)^2$ can be represented by (1.2) in part by writing $\cos^2 \lambda t = (1/2 + 1/2 \cos 2\lambda t)$.

In this light, [1]-[6] discuss systems with essentially a two-frequency parametric excitation. To identify the regions of instability of a beam subjected to a sinusoidal axial force, Elmaraghy and Tabarrok [1] used a discretizing method and approximated the beam motion as having a finite number of modes. In addition to an excitation acting on the linear term as in (1.1), they considered the case with a time-varying coefficient in the damping. Mallik, Kulkarni and Ram [2] investigated a linear system using a Ritz-Galerkin procedure and investigated both one- and two-degree-of-freedom models. Using Galerkin's method, Noah and Hopkins [3] considered the effect of support flexibility on the motion of pipes transporting a pulsating fluid. Their linear equation of motion contained a parametric excitation on the velocity as well as the two-frequency excitation previously mentioned. Noah and

Hopkins [4] examined the stability of the trivial solution for a problem very similar to the one in [3] using a generalized Hill's analysis. Bajaj [5] studied the nonlinear planar motions of articulated tubes with periodic flow through them, and his system involved a cubic nonlinearity as well as the parametric excitation. Barr and McWhannel [6] examined the lateral motions of structures undergoing vertical ground motion. Their single-degree-of-freedom model was linear, contained no damping, and involved a two-frequency parametric excitation with the form of (1.2).

Other references with $M > 2$ in (1.2) are [7]-[9], but in each of these studies certain limitations were placed on the λ_m . In their book, Schmidt and Tondl [7] discussed a very general nonlinear single-degree-of-freedom system. Their parametric excitation contained multiple harmonic components; however, all frequencies were integral multiples of a single frequency, and an external excitation was included in addition to the parametric excitation. Only certain special cases were covered in detail. Watt and Barr [8] studied the stability boundary of a single-degree-of-freedom linear system containing a multifrequency parametric excitation. Their pseudo-random excitation was composed of only frequencies near two times a linear natural frequency of the system. More generally, yet still somewhat restricted, Bogdanoff and Citron [9] presented results from experiments on an inverted pendulum subjected to a multifrequency excitation and compared their results to theoretical predictions. The theoretical predictions were based on a linear ordinary differential equation of motion with constant coefficients. The excitation amplitudes were small, while the frequencies were large, and there were large differences between excitation frequencies.

Most relevant to the present work are [10]-[12]. In [10], MMS was used by Nayfeh to study a two-degree-of-freedom linear system with the identical excitation as in (1.1). He examined three different cases with two simultaneous resonances in each

case. In each resonance, the excitation frequency was either a sum or difference of the two natural frequencies of the system, or one or two times a natural frequency. Nayfeh and Jebril [11] extended Nayfeh's previous study by adding quadratic and cubic nonlinearities to the problem. Once again, four possible cases were examined: (1) principal parametric resonance, (2) the sum of the two natural frequencies near an excitation frequency, (3) the difference of the two natural frequencies near an excitation frequency, and (4) simultaneous principal parametric resonances. Finally, Plaut [12] investigated an air-inflated cylindrical membrane whose internal pressure fluctuated slightly. The fluctuation appeared as a parametric term in the governing equation similar to the excitation in (1.1). Using MMS, he analyzed the single-degree-of-freedom nonlinear system for five resonances: an excitation frequency near one, two, or three times a natural frequency, and the sum or difference of two excitation frequencies near two times a natural frequency.

All of the studies discussed above lack the generality in their mathematical models that is found in (1.1). Often, all nonlinear effects are ignored [1]-[4], [6], [8]-[10]. All of the previous examples consider a finite number of degrees of freedom [1]-[12]. Limitations are frequently placed on the number of excitation frequencies [2]-[7] or on the relationships between the λ_m [6]-[8].

This thesis will partially fill the void in the literature above by providing a general MMS analysis of (1.1), which is an infinite-degree-of-freedom system containing a multifrequency parametric excitation with independent amplitudes, frequencies, and phases. Three resonance conditions will be considered in detail. First, we will study the case when the sum of two excitation frequencies is near twice a natural frequency of the system, $\lambda_s + \lambda_t \simeq 2\omega_q$. Next, the influence of an internal resonance, $\omega_q \simeq 3\omega_r$, on the previous case will be examined. Finally, the effect of the internal resonance $\omega_r \simeq 3\omega_q$ on $\lambda_s + \lambda_t \simeq 2\omega_q$ will be investigated. In each case, plots of response

amplitudes as functions of a detuning parameter and excitation amplitude will be presented. In the first case, the variation of the response amplitude will also be presented as a function of the relative magnitudes of λ_s and λ_r .

Chapter 2

Analysis

To approximate the solution of

$$\begin{aligned} \ddot{u}_n + 2\varepsilon c_n(\varepsilon)\dot{u}_n + \omega_n^2 u_n + 2\varepsilon \sum_{m=1}^M \cos(\lambda_m t + \tau_m) \sum_{j=1}^{\infty} Q_{jn}^m(\varepsilon) u_j \\ + \varepsilon \sum_{j=1}^{\infty} \sum_{k=1}^{\infty} \Lambda_{jkn} u_j u_k + \varepsilon^2 \sum_{j=1}^{\infty} \sum_{k=1}^{\infty} \sum_{l=1}^{\infty} \Gamma_{jkl n} u_j u_k u_l = 0; \quad n = 1, 2, \dots, \end{aligned} \quad (1.1)$$

we introduce the series

$$c_n(\varepsilon) = c_{n1} + \varepsilon c_{n2} + \dots \quad \text{and} \quad Q_{jn}^m(\varepsilon) = Q_{jn1}^m + \varepsilon Q_{jn2}^m + \dots \quad (2.1)$$

for the damping coefficients and parametric excitation amplitudes, respectively, where $c_{nj} \geq 0$ for all j . Following the method of multiple scales [13], we assume that the solution of (1.1) can be expressed as

$$u_n(t; \varepsilon) \simeq u_{n0}(T_0, T_1, T_2, \dots) + \varepsilon u_{n1}(T_0, T_1, T_2, \dots) + \varepsilon^2 u_{n2}(T_0, T_1, T_2, \dots) + \dots \quad (2.2)$$

for $n = 1, 2, \dots$, where t has been replaced by "multiple time scales", i.e.,

$$T_n = \varepsilon^n t. \quad (2.3)$$

Derivatives with respect to time become sums of partial derivatives with respect to the T_n :

$$\frac{d}{dt} = D_0 + \varepsilon D_1 + \varepsilon^2 D_2 + \dots \quad (2.4)$$

$$\frac{d^2}{dt^2} = D_0^2 + 2\varepsilon D_0 D_1 + \varepsilon^2 (2D_0 D_2 + D_1^2) + \dots \quad (2.5)$$

where

$$D_n = \frac{\partial}{\partial T_n}. \quad (2.6)$$

We substitute (2.1), (2.2), (2.4), and (2.5) into (1.1). Because each u_{nj} is independent of ε , the coefficient of each power of ε can be set to zero independently to obtain the governing equations for the u_{nj} . Considering only terms of order ε^2 or less, we obtain

$$O(\varepsilon^0): D_0^2 u_{n0} + \omega_n^2 u_{n0} = 0 \quad (2.7)$$

$$O(\varepsilon^1): D_0^2 u_{n1} + \omega_n^2 u_{n1} = -2(D_0 D_1 + c_{n1} D_0) u_{n0} - 2 \sum_{m=1}^M \cos(\lambda_m T_0 + \tau_m) \sum_{j=1}^{\infty} Q_{jn1}^m u_{j0} - \sum_{j=1}^{\infty} \sum_{k=1}^{\infty} \Lambda_{jkn} u_{j0} u_{k0} \quad (2.8)$$

$$\begin{aligned}
O(\varepsilon^2): \quad D_0^2 u_{n2} + \omega_n^2 u_{n2} = & -2(D_0 D_1 + c_{n1} D_0) u_{n1} \\
& - (2D_0 D_2 + D_1^2 + 2c_{n2} D_0 + 2c_{n1} D_1) u_{n0} \\
& - 2 \sum_{m=1}^M \cos(\lambda_m T_0 + \tau_m) \sum_{j=1}^{\infty} (Q_{jn2}^m u_{j0} + Q_{jn1}^m u_{j1}) \\
& - \sum_{j=1}^{\infty} \sum_{k=1}^{\infty} \Lambda_{jkn}^* u_{j1} u_{k0} - \sum_{j=1}^{\infty} \sum_{k=1}^{\infty} \sum_{l=1}^{\infty} \Gamma_{jkl n} u_{j0} u_{k0} u_{l0}
\end{aligned} \tag{2.9}$$

where

$$\Lambda_{jkn}^* = \Lambda_{jkn} + \Lambda_{kjn}. \tag{2.10}$$

The general solution of (2.7) can be written as

$$u_{n0} = A_n(T_1, T_2, \dots) \exp(i\omega_n T_0) + cc \tag{2.11}$$

where cc denotes the complex conjugate of the preceding terms on the right-hand side of the equation. Substituting (2.11) into (2.8) results in

$$\begin{aligned}
D_0^2 u_{n1} + \omega_n^2 u_{n1} = & -2i\omega_n (D_1 A_n + c_{n1} A_n) \exp(i\omega_n T_0) \\
& - \sum_{j=1}^{\infty} \sum_{m=1}^M Q_{jn1}^m [A_j \exp\{i[(\lambda_m + \omega_j)T_0 + \tau_m]\} + \bar{A}_j \exp\{i[(\lambda_m - \omega_j)T_0 + \tau_m]\}] \\
& - \sum_{j=1}^{\infty} \sum_{k=1}^{\infty} \Lambda_{jkn} A_j \{A_k \exp[i(\omega_j + \omega_k)T_0] + \bar{A}_k \exp[i(\omega_j - \omega_k)T_0]\} + cc
\end{aligned} \tag{2.12}$$

where overbars denote complex conjugates. Small divisors will occur in the solution for u_{n1} if one or more of the following conditions is met (for any j, k, m and n):

$$\omega_n \simeq |\omega_j \pm \omega_k|, \quad \text{including } \omega_n \simeq 2\omega_j; \tag{2.13}$$

$$\omega_n \simeq |\lambda_m \pm \omega_j|, \quad \text{including } 2\omega_n \simeq \lambda_m. \tag{2.14}$$

We consider the case where none of the resonance conditions in (2.13) and (2.14) is met and eliminate the secular terms from u_{n1} by setting

$$c_{n1} = 0 \text{ and } D_1 A_n = 0. \quad (2.15)$$

For convenience we also set

$$c_{n2} = \mu_n, \quad (2.16)$$

and it follows from (2.15) that

$$A_n = A_n(T_2). \quad (2.17)$$

As in the linear case, the approximate solution is the sum of homogeneous and particular parts; however, as explained by Nayfeh and Mook [13], it is unnecessary to include the homogeneous solution in any terms of the expansion except the first. Therefore, the solution of (2.12) is given by

$$\begin{aligned} u_{n1} = & - \sum_{j=1}^{\infty} \sum_{k=1}^{\infty} \Lambda_{jkn} A_j \{ R_{nj k} A_k \exp[i(\omega_j + \omega_k)T_0] + S_{nj k} \bar{A}_k \exp[i(\omega_j - \omega_k)T_0] \} \\ & - \sum_{j=1}^{\infty} \sum_{m=1}^M Q_{jn1}^m [R_{n\lambda j}^m A_j \exp\{i[(\lambda_m + \omega_j)T_0 + \tau_m]\} \\ & + S_{n\lambda j}^m \bar{A}_j \exp\{i[(\lambda_m - \omega_j)T_0 + \tau_m]\}] + cc \end{aligned} \quad (2.18)$$

where

$$R_{njk} = \frac{1}{[\omega_n^2 - (\omega_j + \omega_k)^2]}, \quad S_{njk} = \frac{1}{[\omega_n^2 - (\omega_j - \omega_k)^2]}, \quad (2.19)$$

$$R_{n\lambda j}^m = \frac{1}{[\omega_n^2 - (\lambda_m + \omega_j)^2]}, \quad S_{n\lambda j}^m = \frac{1}{[\omega_n^2 - (\lambda_m - \omega_j)^2]}.$$

Using (2.11) and (2.18) in (2.9), we obtain

$$\begin{aligned} D_0^2 u_{n2} + \omega_n^2 u_{n2} = & -2i\omega_n(D_2 A_n + \mu_n A_n) \exp(i\omega_n T_0) \\ & + \sum_{j=1}^{\infty} \sum_{k=1}^{\infty} \sum_{l=1}^{\infty} \sum_{y=1}^4 (-\Gamma_{jkl n} + \sum_{z=1}^{\infty} \Lambda_{lzn}^* \Lambda_{jkz} \phi_y) \psi_y \exp(iv_y T_0) \\ & + \sum_{j=1}^{\infty} \sum_{k=1}^{\infty} \sum_{l=1}^{\infty} \sum_{m=1}^M \sum_{y=5}^8 \Lambda_{lkn}^* Q_{jl1}^m \phi_y \psi_y \exp[i(v_y T_0 + \eta_y)] \\ & - \sum_{j=1}^{\infty} \sum_{m=1}^M \sum_{y=9}^{10} Q_{jn2}^m \phi_y \psi_y \exp[i(v_y T_0 + \eta_y)] \\ & + \sum_{j=1}^{\infty} \sum_{k=1}^{\infty} \sum_{l=1}^{\infty} \sum_{m=1}^M \sum_{y=11}^{14} Q_{ln1}^m \Lambda_{jkl} \phi_y \psi_y \exp[i(v_y T_0 + \eta_y)] \\ & + \sum_{j=1}^{\infty} \sum_{k=1}^{\infty} \sum_{m=1}^M \sum_{v=1}^M \sum_{y=15}^{18} Q_{kn1}^m Q_{jk1}^v \phi_y \psi_y \exp[i(v_y T_0 + \eta_y)] + cc \end{aligned} \quad (2.20)$$

where ϕ_y , ψ_y , v_y , and η_y are given in Appendix A.

If $Q_{jn1}^m \neq 0$ and $Q_{jn2}^m = 0$, small divisors will occur in the solution for u_{n2} if one or more of the following conditions are met (for any values of j, k, l, m, v and n):

$$\omega_n \simeq |\omega_j \pm \omega_k \pm \omega_l|, \quad \text{including } \omega_n \simeq |\omega_j \pm 2\omega_k|, \quad \omega_n \simeq 3\omega_j, \quad \omega_n \simeq \omega_j; \quad (2.21)$$

$$\omega_n \simeq |\lambda_m \pm \omega_j \pm \omega_k|, \quad \text{including } \omega_n \simeq |\lambda_m \pm 2\omega_j|, \quad \omega_n \simeq \lambda_m, \quad 3\omega_n \simeq \lambda_m; \quad (2.22)$$

$$\omega_n \simeq |\lambda_m \pm \lambda_v \pm \omega_j|, \quad \text{including } \omega_n \simeq |2\lambda_m \pm \omega_j|, \quad 2\omega_n \simeq |\lambda_m \pm \lambda_v|. \quad (2.23)$$

If $Q_{jn1}^m = 0$ and $Q_{jn2}^m \neq 0$, small divisors will occur if (2.14) or (2.21) is satisfied. Because (2.14) has been ruled out, and (2.21) produces small divisors for $Q_{jn1}^m \neq 0$, we will consider the case in which $Q_{jn2}^m = 0$.

Using terms 2-4, 17, and 18 from Appendix A, we eliminate secular terms from u_{n2} by setting

$$-2\omega_n \left\{ i(D_2 A_n + \mu_n A_n) + e_n A_n - 4A_n \sum_{j=1}^{\infty} \alpha_{jn} A_j \bar{A}_j \right\} + \text{Int} + \text{Para} = 0 \quad (2.24)$$

where Int and Para represent terms resulting from internal resonances (involving only ω 's) and parametric resonances (involving λ 's and ω 's), respectively, and

$$\alpha_{jn} = \frac{1}{8\omega_n(1 + \delta_{jn})} \left\{ -\Gamma_{jjnn}^* + \sum_{k=1}^{\infty} [\Lambda_{knn}^* \Lambda_{jjk}^* S_{knn} + \Lambda_{jkn}^* \Lambda_{jnk}^* (R_{kjn} + S_{kjn})] \right\} \quad (2.25)$$

$$e_n = -\frac{1}{2\omega_n} \sum_{j=1}^{\infty} \sum_{m=1}^M (R_{j\lambda n}^m + S_{j\lambda n}^m) Q_{jn1}^m Q_{nj1}^m. \quad (2.26)$$

In (2.25), δ_{jn} is the Kronecker delta, i.e.,

$$\delta_{jn} = \begin{cases} 1 & j = n \\ 0 & j \neq n \end{cases} \quad (2.27)$$

and

$$\Gamma_{jkin}^* = \Gamma_{jkin} + \Gamma_{kjln} + \Gamma_{jlk n} + \Gamma_{kljn} + \Gamma_{ljk n} + \Gamma_{lkjn}. \quad (2.28)$$

Chapter 3

The Case When $\lambda_s + \lambda_t \simeq 2\omega_q$

We will first consider the case when $\lambda_s + \lambda_t \simeq 2\omega_q$ and no other resonances exist. A detuning parameter, σ , is introduced to provide a quantitative measure of the relationship between the frequencies and is defined by

$$\lambda_s + \lambda_t = 2\omega_q + \varepsilon^2 \sigma. \quad (3.1)$$

Using (3.1) with term 16 of Appendix A, we find that secular terms can be eliminated from the solution for u_{n2} if

$$i(D_2 A_n + \mu_n A_n) + e_n A_n - 4A_n \sum_{j=1}^{\infty} \alpha_{jn} A_j \bar{A}_j + \delta_{nq} h_q \bar{A}_q \exp[i(\sigma T_2 + \tau_s + \tau_t)] = 0 \quad (3.2)$$

where α_{jn} can be found from (2.25), e_n from (2.26), and

$$h_q = -\frac{1}{2\omega_q} \sum_{j=1}^{\infty} (S_{j\lambda q}^t Q_{jq1}^s Q_{qj1}^t + S_{j\lambda q}^s Q_{jq1}^t Q_{qj1}^s). \quad (3.3)$$

Using the form

$$A_n(T_2) = \frac{1}{2} a_n(T_2) \exp[i\beta_n(T_2)] \quad (3.4)$$

in (3.2), and separating real and imaginary parts, we obtain for $n \neq q$:

$$a_n' + \mu_n a_n = 0, \quad (3.5)$$

$$a_n(\beta_n' - e_n + \sum_{j=1}^{\infty} \alpha_{jn} a_j^2) = 0, \quad (3.6)$$

and for $n = q$:

$$a_q' + \mu_q a_q + h_q a_q \sin \gamma = 0, \quad (3.7)$$

$$a_q \left[\frac{1}{2} (\sigma - \gamma') - e_q + \sum_{j=1}^{\infty} \alpha_{jq} a_j^2 - h_q \cos \gamma \right] = 0 \quad (3.8)$$

where

$$\gamma = \sigma T_2 + \tau_s + \tau_t - 2\beta_q \quad (3.9)$$

has been defined to produce an autonomous set of equations for the a_n . The solution of (3.5) shows that all a_n for $n \neq q$ decay exponentially with time.

To determine the steady-state response, we put $a_n = 0$ for $n \neq q$, $a_q' = 0$ and $\gamma' = 0$. Then, it follows from (3.7) and (3.8) that

$$a_q(\mu_q + h_q \sin \gamma) = 0 \quad (3.10)$$

$$a_q\left(\frac{1}{2}\sigma - e_q + \alpha_{qq}a_q^2 - h_q \cos \gamma\right) = 0. \quad (3.11)$$

Obviously, a trivial solution, $a_q = 0$, is possible. Nontrivial solutions are also possible with a_q and γ given by

$$a_q^2 = \frac{1}{\alpha_{qq}}\left(e_q - \frac{1}{2}\sigma \pm \sqrt{h_q^2 - \mu_q^2}\right) \quad (3.12)$$

$$\sin \gamma = -\frac{\mu_q}{h_q} \quad (3.13)$$

where (3.13) was obtained by solving (3.10) for $\sin \gamma$, and (3.12) was obtained by solving (3.11) for $\cos \gamma$ and squaring and adding the result and (3.13) to eliminate γ .

Stability of the nontrivial steady-state solutions is determined by "perturbing" the steady-state amplitudes and phases and investigating the behavior of the "perturbations." We let

$$a_q = \tilde{a}_q + \delta a_q \quad (3.14)$$

$$\gamma = \tilde{\gamma} + \delta \gamma \quad (3.15)$$

where \tilde{a}_q is the steady-state amplitude, $\tilde{\gamma}$ is the steady-state phase, and δa_q and $\delta \gamma$ are perturbations of the amplitude and phase, respectively. Substituting (3.14) and (3.15) into (3.7) and (3.8) and using the fact that \tilde{a}_q and $\tilde{\gamma}$ satisfy (3.10) and (3.11) result in the matrix equation

$$\begin{Bmatrix} \delta a_q' \\ \delta \gamma' \end{Bmatrix} = [M] \begin{Bmatrix} \delta a_q \\ \delta \gamma \end{Bmatrix} \quad (3.16)$$

where

$$[M] = \begin{bmatrix} 0 & -h_q \tilde{a}_q \cos \tilde{\gamma} \\ 2\alpha_{qq} \tilde{a}_q & -\mu_q \end{bmatrix}. \quad (3.17)$$

Solutions for δa_q and $\delta \gamma$ are of the form

$$\delta a_q = C_1 e^{\lambda_1 T_2} + C_2 e^{\lambda_2 T_2} \quad (3.18)$$

$$\delta \gamma = C_3 e^{\lambda_1 T_2} + C_4 e^{\lambda_2 T_2} \quad (3.19)$$

where λ_1 and λ_2 are the eigenvalues of $[M]$, the C_n are constants of integration, and

$$\lambda_1, \lambda_2 = \frac{-\mu_q \pm \sqrt{8\alpha_{qq} h_q \tilde{a}_q^2 \cos \tilde{\gamma}}}{2}. \quad (3.20)$$

If either λ_1 or λ_2 has a positive real part, the perturbations grow, and the solution is unstable. On the other hand, if both λ_1 and λ_2 have negative real parts, the perturbations decay to zero, and the solution is stable.

Stability of the trivial solution may also be determined by substituting (3.14) and (3.15) into (3.7) and (3.8) and then letting $\tilde{a}_q = 0$. This results in the governing equations

$$\delta a_q' = -(\mu_q + h_q \sin \tilde{\gamma}) \delta a_q \quad (3.21)$$

$$\left(\frac{1}{2} \sigma - e_q - h_q \cos \tilde{\gamma}\right) \delta a_q = 0. \quad (3.22)$$

For a nonzero perturbation, $\delta a_q \neq 0$, $\tilde{\gamma}$ can be found from (3.22), and this value is used in (3.21). If $(\mu_q + h_q \sin \tilde{\gamma}) > 0$, the trivial solution is stable, and if $(\mu_q + h_q \sin \tilde{\gamma}) < 0$, the trivial solution is unstable. Numerical studies have shown that $(\mu_q + h_q \sin \tilde{\gamma})$ is greater than zero for small excitation amplitudes. At bifurcation points, $(\mu_q + h_q \sin \tilde{\gamma})$ equals zero, and the stability property of the trivial solution changes at these points.

Alternatively, the stability of the trivial solution may be obtained by letting

$$A_q = \tilde{A}_q + \delta A_q \quad (3.23)$$

and substituting into (3.2). For the trivial solution, $\tilde{A}_q = 0$ and we write

$$\delta A_q = (p + iq) \exp\left[i \frac{1}{2} (\sigma T_2 + \tau_s + \tau_t)\right]. \quad (3.24)$$

Using (3.24) in (3.2) and separating real and imaginary parts gives the governing equations for p and q:

$$\begin{Bmatrix} p' \\ q' \end{Bmatrix} = [T] \begin{Bmatrix} p \\ q \end{Bmatrix} \quad (3.25)$$

where

$$[T] = \begin{bmatrix} -\mu_q & h_q - e_q + \frac{1}{2} \sigma \\ h_q + e_q - \frac{1}{2} \sigma & -\mu_q \end{bmatrix}. \quad (3.26)$$

As for the nontrivial solutions, the eigenvalues of [T] determine the stability properties of the trivial solution. The eigenvalues of [T] are

$$\lambda_1, \lambda_2 = -\mu_q \pm \sqrt{h_q^2 - (e_q - \frac{1}{2} \sigma)^2}. \quad (3.27)$$

Stability of the trivial solution changes at the points where $(h_q^2 - \mu_q^2)^2 = (e_q - \sigma/2)^2$, and these are also the points where the nontrivial solutions bifurcate from the trivial solution. The two methods described for finding the stability of the trivial solution agree completely, and both indicate that the stability of the trivial solution changes at the bifurcation points.

Frequency-response curves (plots of response amplitude as a function of detuning parameter) can have either of the forms shown in Figure 1, hardening behavior when $\alpha_{qq} < 0$ as shown in part (a) or softening behavior when $\alpha_{qq} > 0$ as shown in part (b). The maximum response does not occur when the resonance is perfectly tuned, i.e., $\sigma = 0$, as would be expected in the linear approximation. For $\alpha_{qq} > 0$, the maximum response occurs when $\lambda_s + \lambda_t$ is less than $2\omega_q$, and for $\alpha_{qq} < 0$, the maximum response occurs for $\lambda_s + \lambda_t$ greater than $2\omega_q$. As damping increases, the curves approach each other, and the values on the abscissa are $\sigma = 2(e_q \pm \sqrt{h_q^2 - \mu_q^2})$. The curves will not close as σ is increased in part (a) or decreased in part (b) because the MMS analysis has only been carried to order ε^2 , and thus this analysis is only valid for a small range of σ near perfect tuning. Solid curves in the figures indicate stable steady-state solutions, while dashed curves represent unstable solutions.

Jumps can be seen in both Figures 1(a) and (b). Consider initial conditions which are near the trivial solution for σ sufficiently positive in part (a). The trivial solution is stable in this region, and, as σ is decreased, the response will stay near $a_q = 0$. When σ reaches the bifurcation point, however, the trivial solution is no longer stable, and the response amplitude will "jump" up to the stable nontrivial solution. As σ is decreased further, the response will follow the stable solution curve until the response becomes trivial again. A similar response can be seen in part (b) by choosing initial conditions near the trivial solution, beginning with a sufficiently

negative value of σ and slowly increasing σ until the bifurcation point where the response amplitude will jump to the stable nontrivial solution as σ is increased further. More increase in σ will result in a smooth decrease in the response along the stable solution curve to the trivial solution. These jumps will only be seen for the conditions described above. If initial conditions are chosen in part (a) for a large σ such that the response begins on the nontrivial solution, a_q will smoothly decrease along the nontrivial solution curve to the trivial solution. The same steady response would be seen for large initial conditions and small σ as σ is increased in part (b). Any initial conditions for sufficiently negative σ in part (a) would decay to the trivial solution, and as σ is increased, the response would follow the stable solution curve. Similarly, any initial conditions for σ very large in part (b) would decrease to the trivial solution and the response would follow the continuous stable solution curve as σ is decreased.

In order to illustrate the variation of the response amplitude, a_q , as a function of the excitation amplitudes, we consider the case when all excitation amplitudes are zero except Q_{qq1}^s and Q_{qq1}^t , which are equal and denoted by Q , i.e.,

$$Q = Q_{qq1}^s = Q_{qq1}^t. \quad (3.28)$$

Then, using (3.1) and (3.28) in (2.26) and (3.3), we can write (to order ε^2):

$$e_q = -k_1 Q^2, \quad h_q = -k_2 Q^2 \quad (3.29)$$

where

$$k_1 = \frac{2(\lambda_s^2 + 4\lambda_s\lambda_t + \lambda_t^2)}{\lambda_s\lambda_t(\lambda_s + \lambda_t)(\lambda_s + 2\lambda_t)(2\lambda_s + \lambda_t)}$$

and

$$(3.30)$$

$$k_2 = \frac{2}{\lambda_s \lambda_t (\lambda_s + \lambda_t)}$$

with $k_2 > k_1 > 0$. Also, we define

$$k_3 = k_2 - k_1 > 0$$

and

(3.31)

$$k_4 = k_1 + k_2 > 0.$$

We will first consider the undamped case, $\mu_q = 0$, while all other μ_n remain greater than 0. Then (3.12) with (3.28)-(3.31) yields the solutions

$$a_q^2 = \frac{1}{\alpha_{qq}} (k_3 Q^2 - \frac{1}{2} \sigma), \quad a_q^2 = -\frac{1}{\alpha_{qq}} (k_4 Q^2 + \frac{1}{2} \sigma). \quad (3.32)$$

If $\sigma = 0$, a_q is directly proportional to $|Q|$ as shown in Figure 2(a). Figure 2(b) is applicable if $\sigma > 0$ and $\alpha_{qq} > 0$ or $\sigma < 0$ and $\alpha_{qq} < 0$. The value of Q at the bifurcation point is $Q = \sqrt{\sigma/(2k_3)}$ in the former case and $Q = \sqrt{-\sigma/(2k_4)}$ in the latter. The behavior of a_q as a function of Q when σ and α_{qq} are of opposite signs can be seen in Figure 2(c). For the case when $\alpha_{qq} > 0$ and $\sigma < 0$, the value of Q at the bifurcation point is $Q = \sqrt{-\sigma/(2k_4)}$. When $\alpha_{qq} < 0$ and $\sigma > 0$, the value of Q at the bifurcation point is $Q = \sqrt{\sigma/(2k_3)}$. For both cases, the nontrivial value of a_q where $Q = 0$ is $a_q = \sqrt{-\sigma/(2\alpha_{qq})}$. In all the cases shown, the stable solutions grow as Q is increased.

In the damped case, $\mu_q > 0$, (3.12) becomes

$$a_q^2 = \frac{1}{\alpha_{qq}} \left(-k_1 Q^2 - \frac{1}{2} \sigma \pm \sqrt{k_2^2 Q^4 - \mu_q^2} \right) \quad (3.33)$$

with the use of (3.28)-(3.30). Figure 2(d) shows the variation of a_q with Q when Q_A , the value of Q at the turning point, is less than Q_B , the value of Q at the bifurcation point, and a_A^2 , the value of a_q^2 at the turning point, is positive, where

$$Q_A = \sqrt{\frac{\mu_q}{k_2}}, \quad Q_B^2 = \frac{k_1 \sigma + \sqrt{k_2^2 \sigma^2 + 4\mu_q^2(k_2^2 - k_1^2)}}{2(k_2^2 - k_1^2)} \quad (3.34)$$

$$a_A^2 = -\frac{1}{2k_2 \alpha_{qq}} (2k_1 \mu_q + \sigma k_2).$$

The transition from stable to unstable solutions occurs at the point of vertical tangency. Figure 2(e) illustrates the behavior of a_q as a function of Q when a_A^2 is negative and only one solution is possible.

A jump in the response amplitude can be seen in Figure 2(c). Initial conditions near the trivial solution for small Q will decay to the trivial solution, and as Q is increased past the bifurcation point, the response will jump to the stable nontrivial solution. Jumps can be observed for both increasing and decreasing Q in part (d). For small Q and small initial conditions, the response will continue to be trivial as Q is increased up to the bifurcation. At this point, the response will jump to the nontrivial solution. The response for any initial conditions at a large Q will converge to the stable nontrivial solution and continue along this curve to the vertical tangent

where a_q will jump down to the trivial solution. No jumps would be seen in the response for parts (a), (b), and (e).

The response amplitude, a_q , also depends upon the relative magnitudes of the excitation frequencies, λ_s and λ_t . We define

$$\Gamma = \frac{\lambda_s}{2\omega_q} \quad (3.35)$$

and look at the variation of a_q with Γ to illustrate this dependence. Substituting (3.35) into (3.33) gives

$$a_q^2 = \frac{1}{\alpha_{qq}} \left[\frac{(2\Gamma^2 - 2\Gamma - 1)Q^2}{4\omega_q^3\Gamma(2 - \Gamma)(1 - \Gamma^2)} - \frac{1}{2}\sigma \pm \sqrt{\frac{Q^4}{16\omega_q^6\Gamma^2(1 - \Gamma)^2} - \mu_q^2} \right]. \quad (3.36)$$

Near $\Gamma = 0$, 0.5, or 1, (3.36) is not valid because other resonances exist. Figure 3 shows some possibilities of the behavior of a_q with Γ , with $\mu_q = 0$, $\alpha_{qq} < 0$ in part (a), $\mu_q > 0$, $\alpha_{qq} > 0$ in (b) and $\mu_q > 0$, $\alpha_{qq} < 0$ in (c). Jumps would be observed in the response in part (c), while none would occur in parts (a) and (b).

Next, we will continue to assume that Q_{qq1}^s and Q_{qq1}^t are the only nonzero excitation amplitudes; however, we will fix one and vary the other. Let

$$Q_s = Q_{qq1}^s, \quad Q_t = Q_{qq1}^t, \quad (3.37)$$

and assume Q_t is fixed. Now (2.26) and (3.3) can be written as

$$e_q = -k_5 - k_6 Q_s^2, \quad h_q = -k_7 Q_s \quad (3.38)$$

where

$$k_5 = \frac{2Q_t^2}{(\lambda_s + \lambda_t)(\lambda_s + 2\lambda_t)\lambda_s}, \quad k_6 = \frac{2}{(\lambda_s + \lambda_t)(\lambda_t + 2\lambda_s)\lambda_t}$$

and

(3.39)

$$k_7 = \frac{2Q_t}{(\lambda_s + \lambda_t)\lambda_s\lambda_t}.$$

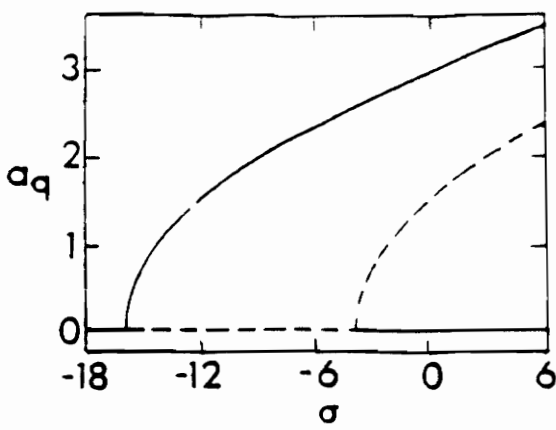
Using (3.36) and (3.37), (3.12) can be written as

$$a_q^2 = -\frac{1}{2\alpha_{qq}} (2k_5 + 2k_6Q_s^2 + \sigma \pm 2\sqrt{k_7^2Q_s^2 - \mu_q^2}). \quad (3.40)$$

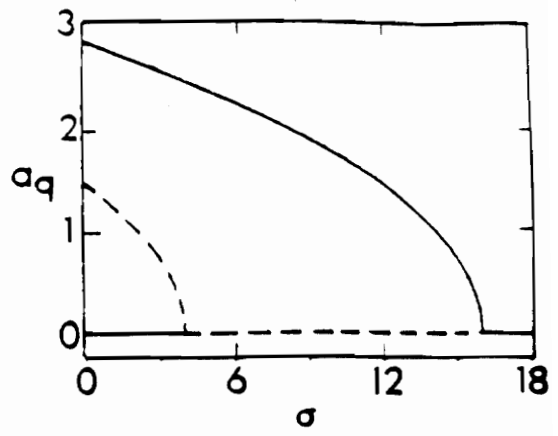
Figure 4 shows some examples of the variation of a_q with Q_s , where $Q = Q_s$. In Figure 4(a), one stable nontrivial solution is present for small values of Q . A second nontrivial solution is possible for larger values of Q ; however, it is always unstable. The trivial solution is unstable in the region where only one solution is present but becomes stable when the second nontrivial solution appears. In Figure 4(b), no nontrivial solutions are possible for very small values of Q , and two solutions are present near the first bifurcation point. A lower nontrivial solution appears for Q sufficiently large. As in Figure 4(a), the lower nontrivial solution is always unstable, and the trivial solution is stable when no nontrivial solutions or two nontrivial solutions are present. The trivial solution is unstable in the region where only one nontrivial solution is possible. A similar case to Figure 4(b) is seen in Figure 4(c); however, there is only one bifurcation point, and the area where two nontrivial solutions exist, near the bifurcation, has expanded. The stability of the trivial solution is the same as that in Figure 4(b). In Figure 4(d), one nontrivial solution is possible for a limited range of Q , and it is stable. Outside this range, only the trivial solution

is possible. Jumps can be observed in the response in parts (a)-(c) with only smooth transitions in part (d).

In this chapter we have examined the resonance that occurs when the sum of two parametric excitation frequencies is near two times a natural frequency of the system, i.e., $\lambda_s + \lambda_t \simeq 2\omega_q$. In each of the cases shown, all stability changes occur at bifurcation points or points of vertical tangency. At most, two nontrivial solutions are possible for the cases shown here. In the regions where two stable solutions are present, initial conditions determine which response will occur.



(a)



(b)

Figure 1. Frequency-response curves: In (a), $\mu_q = 0.1$, $\alpha_{qq} = -1$, $e_q = -5$, $h_q = 3$. In (b), $\mu_q = 0.1$, $\alpha_{qq} = 1$, $e_q = 5$, $h_q = 3$.

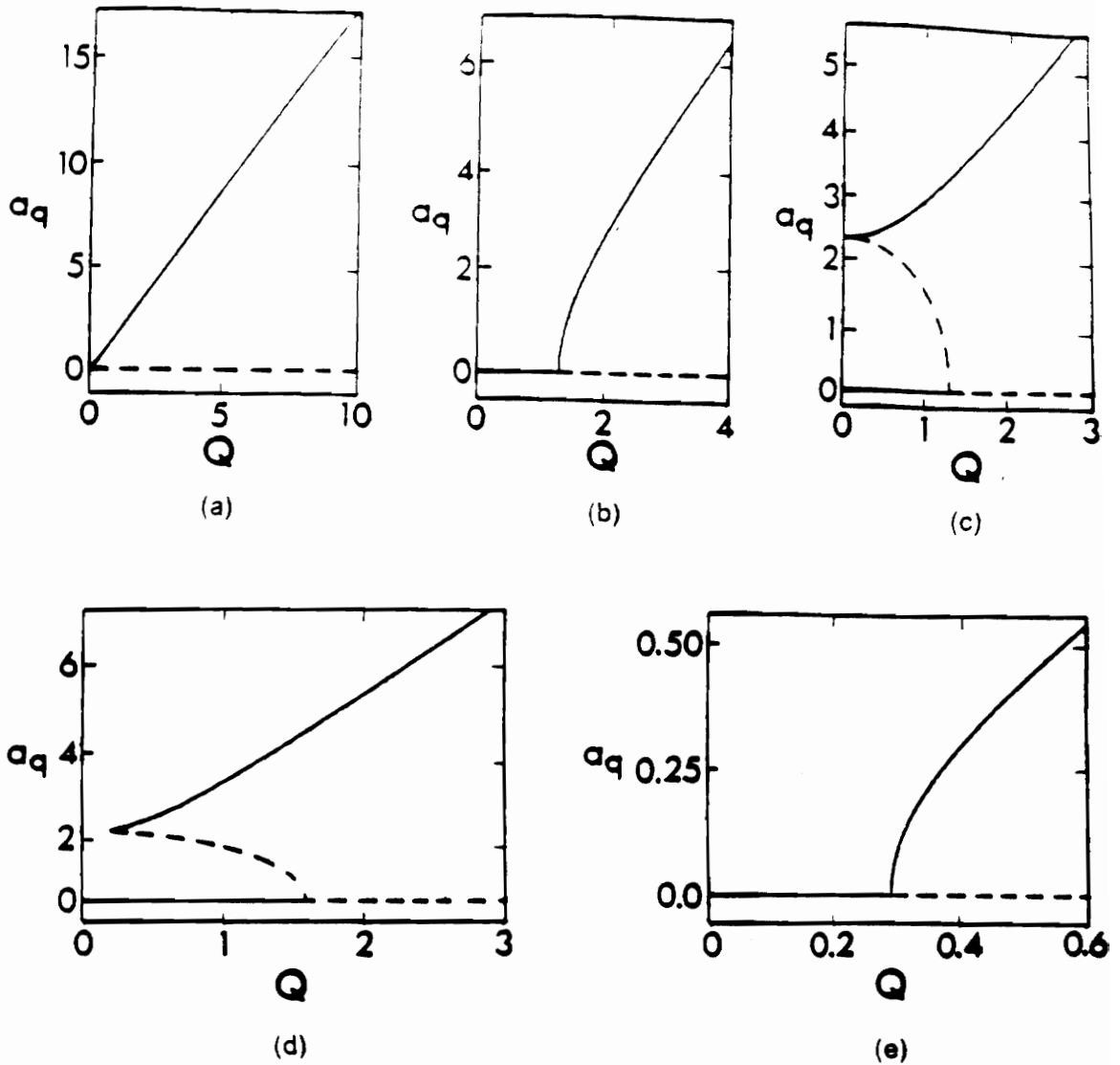


Figure 2. Response amplitude as a function of excitation amplitude: In (a), $\mu_q = 0$, $\alpha_{qq} = 1$, $\sigma = 0$, $k_3 = 3$. In (b), $\mu_q = 0$, $\alpha_{qq} = 1$, $\sigma = 10$, $k_3 = 3$. In (c), $\mu_q = 0$, $\alpha_{qq} = 1$, $\sigma = -10$, $k_4 = 3$. In (d), $\mu_q = 0.5$, $\alpha_{qq} = -1$, $\sigma = 5$, $k_1 = 2$, $k_2 = 3$. In (e), $\mu_q = 0.1$, $\alpha_{qq} = 1$, $\sigma = 0.1333$, $k_1 = 2$, $k_2 = 3$.

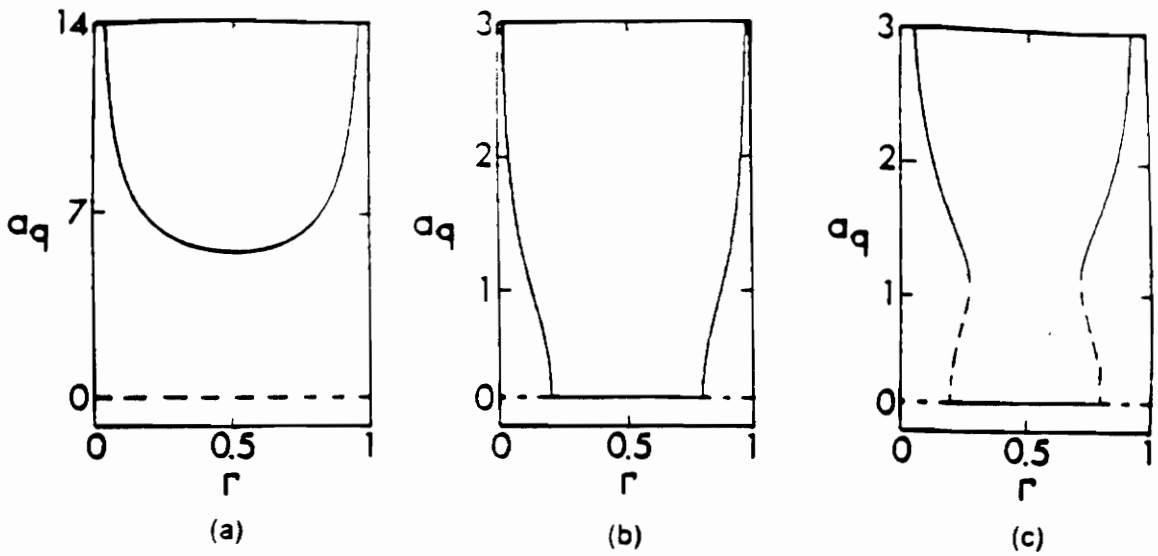


Figure 3. Response amplitude as a function of Γ : In (a), $\mu_q = 0$, $\alpha_{qq} = -1$, $\sigma = 0$, $Q = 4$, $\omega_q = 1$. In (b), $\mu_1 = 1.25$, $\alpha_{qq} = 1$, $\sigma = 0$, $Q = 1$, $\omega_q = 1$. In (c), $\mu_q = 1.25$, $\alpha_{qq} = -1$, $\sigma = 0$, $Q = 1$, $\omega_q = 1$.

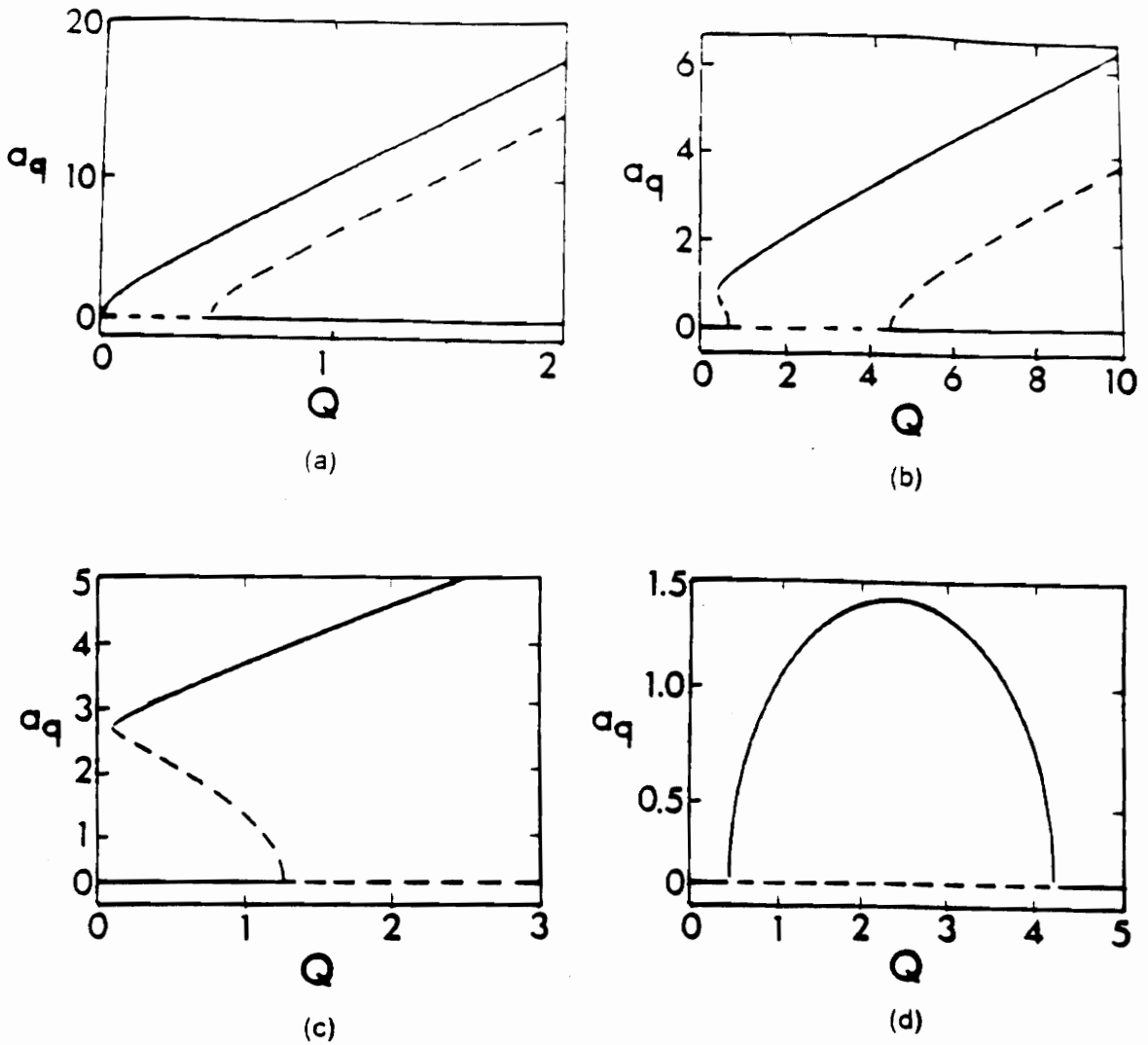


Figure 4. Response amplitude as a function of excitation amplitude: In (a), $\mu_q = 0$, $\alpha_{qq} = -1$, $\sigma = -2.1333$, $Q_t = 2$, $\lambda_s = 1.5$, $\lambda_t = 0.5$. In (b), $\mu_q = 0.5$, $\alpha_{qq} = -1$, $\sigma = 0$, $Q_t = 1$, $\lambda_s = 0.5$, $\lambda_t = 1.5$. In (c), $\mu_q = 0.5$, $\alpha_{qq} = -1$, $\sigma = 3$, $Q_t = 4$, $\lambda_s = 1.5$, $\lambda_t = 0.5$. In (d), $\mu_q = 0$, $\alpha_{qq} = 1$, $\sigma = 0$, $Q_t = 2$, $\lambda_s = 1.5$, $\lambda_t = 0.5$.

Chapter 4

The Case When

$$\lambda_s + \lambda_t \simeq 2\omega_q \text{ and } \omega_q \simeq 3\omega_r$$

We now examine the effect of an internal resonance, $\omega_q \simeq 3\omega_r$, on the previous case where $\lambda_s + \lambda_t \simeq 2\omega_q$. Again we assume no other resonances exist. Detuning parameters σ_1 and σ_2 are defined by

$$\lambda_s + \lambda_t = 2\omega_q + \varepsilon^2 \sigma_1 \quad (4.1)$$

and

$$\omega_q = 3\omega_r + \varepsilon^2 \sigma_2. \quad (4.2)$$

Using (4.1), (4.2) and terms 1-4 and 16 of Appendix A, (2.24) can be written as

$$\begin{aligned}
& i(D_2 A_n + \mu_n A_n) + e_n A_n - 4A_n \sum_{j=1}^{\infty} \alpha_{jn} A_j \bar{A}_j + \delta_{nq} h_q \bar{A}_q \exp[i(\sigma_1 T_2 + \tau_s + \tau_t)] \\
& - 4\delta_{nq} W_{rq} A_r^3 \exp(-i\sigma_2 T_2) - 4\delta_{nr} V_{qr} A_q \bar{A}_r^2 \exp(i\sigma_2 T_2) = 0
\end{aligned} \tag{4.3}$$

where α_{jn} is given by (2.25), e_n by (2.26), h_q by (3.3),

$$W_{rq} = \frac{1}{8\omega_q} \left[-\Gamma_{rrrq} + \sum_{j=1}^{\infty} \Lambda_{jrq}^* \Lambda_{rrj} R_{jrr} \right] \tag{4.4}$$

and

$$V_{qr} = \frac{1}{8\omega_r} \left[-\frac{1}{2} \Gamma_{qrrr} + \sum_{j=1}^{\infty} (\Lambda_{jrr}^* \Lambda_{qrj} S_{jqr} + \Lambda_{jqr}^* \Lambda_{rrj} R_{jrr}) \right] \tag{4.5}$$

where Γ_{jkn}^* is defined by (2.28) and Λ_{jkn}^* by (2.10).

Substituting (3.4) into (4.3) results in (3.5) and (3.6) for $n \neq q$ or r , and

$$a_q' + \mu_q a_q + h_q a_q \sin \gamma_1 + W_{rq} a_r^3 \sin \gamma_2 = 0, \tag{4.6}$$

$$a_q \left(\beta_q' - e_q + \sum_{j=1}^{\infty} \alpha_{jq} a_j^2 - h_q \cos \gamma_1 \right) + W_{rq} a_r^3 \cos \gamma_2 = 0, \tag{4.7}$$

$$a_r' + \mu_r a_r - V_{qr} a_q a_r^2 \sin \gamma_2 = 0, \tag{4.8}$$

$$a_r \left(\beta_r' - e_r + \sum_{j=1}^{\infty} \alpha_{jr} a_j^2 + V_{qr} a_q a_r \cos \gamma_2 \right) = 0 \tag{4.9}$$

for $n = q$ and r where

$$\gamma_1 = \sigma_1 T_2 + \tau_s + \tau_t - 2\beta_q \quad (4.10)$$

and

$$\gamma_2 = \sigma_2 T_2 + \beta_q - 3\beta_r. \quad (4.11)$$

In the steady state, $a_n' = 0$, $\gamma_1' = 0$, and $\gamma_2' = 0$. As before, all a_n for $n \neq q$ or r are zero, and the nontrivial steady-state solutions for a_q , a_r , γ_1 , and γ_2 are governed by

$$a_q(\mu_q + h_q \sin \gamma_1) + W_{rq} a_r^3 \sin \gamma_2 = 0, \quad (4.12)$$

$$a_q(\xi_1 - h_q \cos \gamma_1) + W_{rq} a_r^3 \cos \gamma_2 = 0, \quad (4.13)$$

$$a_r(\mu_r - V_{qr} a_q a_r \sin \gamma_2) = 0, \quad (4.14)$$

$$a_r(\xi_2 + \xi_3 + V_{qr} a_q a_r \cos \gamma_2) = 0, \quad (4.15)$$

where

$$\xi_1 = \frac{1}{2} \sigma_1 - e_q + \alpha_{qq} a_q^2 + \alpha_{rq} a_r^2, \quad (4.16)$$

$$\xi_2 = \alpha_{qr} a_q^2 + \alpha_{rr} a_r^2, \quad (4.17)$$

$$\xi_3 = \frac{1}{6} (\sigma_1 + 2\sigma_2) - e_r. \quad (4.18)$$

A trivial solution, $a_q = a_r = 0$, exists along with nontrivial solutions. One possibility is $a_r = 0$ and $a_q \neq 0$ which reduces to the case studied in the previous section where no

internal resonance was present. Nontrivial solutions with $a_r \neq 0$ and $a_q \neq 0$ also exist for certain parameter ranges.

The stability of the steady-state solutions is determined by the procedure described in the previous chapter. We let

$$a_q = \tilde{a}_q + \delta a_q \quad (4.19)$$

$$a_r = \tilde{a}_r + \delta a_r \quad (4.20)$$

$$\gamma_1 = \tilde{\gamma}_1 + \delta \gamma_1 \quad (4.21)$$

$$\gamma_2 = \tilde{\gamma}_2 + \delta \gamma_2. \quad (4.22)$$

Using (4.19)-(4.22) in (4.6)-(4.9) and taking advantage of (4.12)-(4.15) gives

$$\begin{array}{ccc} \delta a_q' & & \delta a_q \\ \delta a_r' & & \delta a_r \\ \delta \gamma_1' & & \delta \gamma_1 \\ \delta \gamma_2' & & \delta \gamma_2 \end{array} = [M] \quad (4.23)$$

where the elements of [M] are

$$M_{11} = -(\mu_q + h_q \sin \tilde{\gamma}_1)$$

$$M_{12} = -3W_{rq} \tilde{a}_r^2 \sin \tilde{\gamma}_2$$

$$M_{13} = -h_q \tilde{a}_q \cos \tilde{\gamma}_1$$

$$M_{14} = -W_{rq} \tilde{a}_r^3 \cos \tilde{\gamma}_2$$

$$M_{21} = V_{qr} \tilde{a}_r^2 \sin \tilde{\gamma}_2$$

$$M_{22} = 2V_{qr} \tilde{a}_q \tilde{a}_r \sin \tilde{\gamma}_2 - \mu_r$$

$$M_{23} = 0$$

$$M_{24} = V_{qr} \tilde{a}_q \tilde{a}_r^2 \cos \tilde{\gamma}_2 \quad (4.24)$$

$$M_{31} = 2 \left(2\alpha_{qq} \tilde{a}_q - \frac{W_{rq} \tilde{a}_r^3}{\tilde{a}_q^2} \cos \tilde{\gamma}_2 \right)$$

$$M_{32} = 2 \left(\frac{3W_{rq} \tilde{a}_r^2}{\tilde{a}_q} \cos \tilde{\gamma}_2 + 2\alpha_{rq} \tilde{a}_r \right)$$

$$M_{33} = 2h_q \sin \tilde{\gamma}_1$$

$$M_{34} = \frac{-W_{rq} \tilde{a}_r^3}{\tilde{a}_q} \sin \tilde{\gamma}_2$$

$$M_{41} = \frac{W_{rq} \tilde{a}_r^3}{\tilde{a}_q^2} \cos \tilde{\gamma}_2 + 2(3\alpha_{qr} - \alpha_{qq}) \tilde{a}_q + 3V_{qr} \tilde{a}_r \cos \tilde{\gamma}_2$$

$$M_{42} = \frac{-3W_{rq} \tilde{a}_r^2}{\tilde{a}_q} \cos \tilde{\gamma}_2 + 2(3\alpha_{rr} - \alpha_{rq}) \tilde{a}_r + 3V_{qr} \tilde{a}_q \cos \tilde{\gamma}_2$$

$$M_{43} = -h_q \sin \tilde{\gamma}_1$$

$$M_{44} = -3V_{qr} \tilde{a}_q \tilde{a}_r \sin \tilde{\gamma}_2 + \frac{W_{rq} \tilde{a}_r^3}{\tilde{a}_q} \sin \tilde{\gamma}_2.$$

The solutions for δa_q , δa_r , $\delta \gamma_r$, and $\delta \gamma_2$ can be written in the form

$$\delta a_q = \sum_{j=1}^4 C_{1j} e^{\lambda_j T_2} \quad (4.25)$$

$$\delta a_r = \sum_{j=1}^4 C_{2j} e^{\lambda_j T_2} \quad (4.26)$$

$$\delta \gamma_1 = \sum_{j=1}^4 C_{3j} e^{\lambda_j T_2} \quad (4.27)$$

$$\delta \gamma_2 = \sum_{j=1}^4 C_{4j} e^{\lambda_j T_2} \quad (4.28)$$

where the λ_j are eigenvalues of $[M]$, and the C_{ij} are constants of integration. As before, any eigenvalue with a positive real part indicates an unstable solution, and if the real parts of all the λ_j are less than zero, the solution is stable.

Stability of the trivial solution may also be determined by substituting (4.19)-(4.22) into (4.6)-(4.9) and using (4.12)-(4.15); however, $\tilde{a}_q = \tilde{a}_r = 0$, and we can no longer divide by \tilde{a}_q and \tilde{a}_r to get (4.24). In this case, the governing equations for δa_q and δa_r are

$$\delta a_q' = -(\mu_q + h_q \sin \tilde{\gamma}_1) \delta a_q \quad (4.29)$$

$$\delta a_r' = -\mu_r \delta a_r \quad (4.30)$$

where γ_1 is arbitrary for the trivial solution. Equation (4.29) is identical to (3.21) and indicates the same stability properties for $\tilde{a}_q = 0$ as in Chapter 3. When $(\mu_q + h_q \sin \tilde{\gamma}_1) = 0$, a_q bifurcates from the trivial solution, and the trivial solution changes its stability character as in Chapter 3. It is assumed that $\mu_r > 0$, and the solution of (4.30) shows that δa_r always decays and $\tilde{a}_r = 0$ is stable. No nontrivial a_r solutions bifurcate from $a_r = 0$. For certain ranges of excitation amplitude, initial conditions near $a_q = a_r = 0$ will result in the growth of the q^{th} mode while the r^{th} mode remains small.

The alternative procedure described in Chapter 3 may also be used to determine the stability of the trivial solution. For $n = q$, (3.25) is obtained with $[T]$ again given by (3.26). The stability of the A_q trivial solution is then the same as that of the trivial solution in Chapter 3. For $n = r$, let

$$A_r = \tilde{A}_r + \delta A_r, \quad (4.31)$$

substitute (4.31) into (4.3), let $\tilde{A}_r = 0$, and write

$$\delta A_r = (p_r + iq_r) \exp\left[i \frac{1}{2} (\sigma_1 T_2 + \tau_s + \tau_t)\right]. \quad (4.32)$$

Using (4.32) in (4.3) and separating real and imaginary parts results in

$$\begin{Bmatrix} p_r' \\ q_r' \end{Bmatrix} = [T_r] \begin{Bmatrix} p_r \\ q_r \end{Bmatrix} \quad (4.33)$$

where

$$[T_r] = \begin{bmatrix} -\mu_r & -e_r \\ e_r & -\mu_r \end{bmatrix}. \quad (4.34)$$

The eigenvalues of [T,] are

$$\lambda_1, \lambda_2 = -\mu_r \pm ie_r \quad (4.35)$$

indicating that the A, trivial solution is always stable, because the real parts of the eigenvalues of [T,] are always negative. As expected, the two methods for determining the stability of the trivial solution produce the same results and are equivalent.

When $a_q \neq 0$, $a_r \neq 0$, and $\sin \gamma_2 \neq 0$, we can solve (4.14) to obtain

$$a_q = \frac{\mu_r}{a_r V_{qr} \sin \gamma_2}. \quad (4.36)$$

Using (4.36) in (4.15) leads to

$$a_r^2 = \frac{-B \pm \sqrt{B^2 - 4AC}}{2A} \quad (4.37)$$

where

$$A = \alpha_{rr} V_{qr}^2 \sin^2 \gamma_2, \quad B = (\mu_r \cot \gamma_2 + \xi_3) V_{qr}^2 \sin^2 \gamma_2,$$

and (4.38)

$$C = \alpha_{qr} \mu_r^2.$$

Solving (4.12) for $\sin \gamma_1$ and (4.13) for $\cos \gamma_1$ and then squaring and adding the results eliminates γ_1 and yields

$$a_q^2 h_q^2 = (a_q \mu_q + W_{rq} a_r^3 \sin \gamma_2)^2 + (a_q \xi_1 + W_{rq} a_r^3 \cos \gamma_2)^2. \quad (4.39)$$

Again, we will consider the case (3.28) and assume all other excitation amplitudes are zero. Using (3.29) in (4.39) and solving for Q^2 results in

$$Q^2 = \frac{-E \pm \sqrt{E^2 - 4DF}}{2D} \quad (4.40)$$

where

$$D = k_2^2 - k_1^2, \quad E = -2k_1G - \frac{2W_{rq}a_r^3k_1 \cos \gamma_2}{a_q},$$

and

(4.41)

$$F = -\mu_q^2 - G^2 - \frac{W_{rq}^2 a_r^6}{a_q^2} - \frac{2W_{rq}a_r^3}{a_q} (\mu_q \sin \gamma_2 + G \cos \gamma_2).$$

In (4.41),

$$G = \frac{1}{2} \sigma_1 + \alpha_{qq} a_q^2 + \alpha_{rq} a_r^2. \quad (4.42)$$

To determine the behavior of the response amplitudes, a_q and a_r , as functions of Q , we specify σ_1 and σ_2 , and vary γ_2 from 0 to 2π . For each value of γ_2 , a_r is found from (4.37), a_q from (4.36), and Q from (4.40). Frequency-response curves can be obtained by fixing Q and σ_2 , varying σ_1 , and solving (4.37), (4.36), and (4.40) numerically for γ_2 , a_r , and a_q .

Numerical results are presented in Figures 5 and 6, where a_q and a_r are shown as functions of σ_1 and Q , respectively. In both cases, there are a trivial solution ($a_r = a_q = 0$), nontrivial solutions where $a_q \neq 0$ and $a_r = 0$, and finally, nontrivial

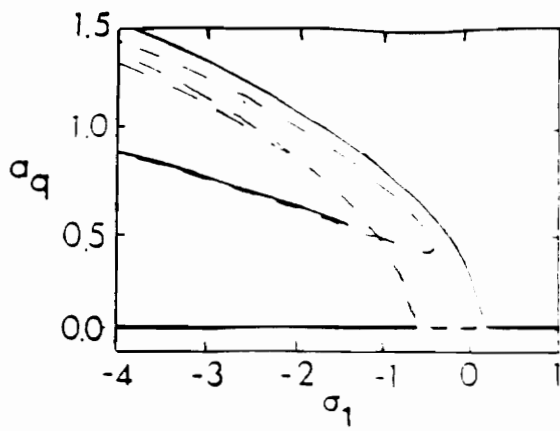
solutions where both a_q and a_r are nonzero ($a_r \neq 0$, $a_q \neq 0$). For the case when $a_q \neq 0$ and $a_r = 0$, a_q bifurcates from the trivial solution, resulting in regions of instability of the a_q trivial solution; however, no nontrivial solutions bifurcate from the trivial solution $a_r = 0$, and small perturbations of a_r from $a_r = 0$ do not grow large.

Consider the solutions with nonzero a_r and a_q . In this case, no solutions bifurcate from the trivial solution, and in Figures 5(a) and (b), there are two branches. One is unstable, while the other has a stable portion for σ_1 sufficiently negative. In Figures 5(c) and (d) the response is shown for a larger value of Q , and a third branch appears on the right which has a stable portion. As Q is increased further, the right branch seems to meet the middle one and the gap between them disappears. As shown in Figures 5(e) and (f), there are three solutions again, but now two are unstable, while the third contains a region of instability in the center and stable solutions on each end. For clarity, Figure 5 is repeated in Figure 6 with unstable solutions removed and corresponding solutions marked.

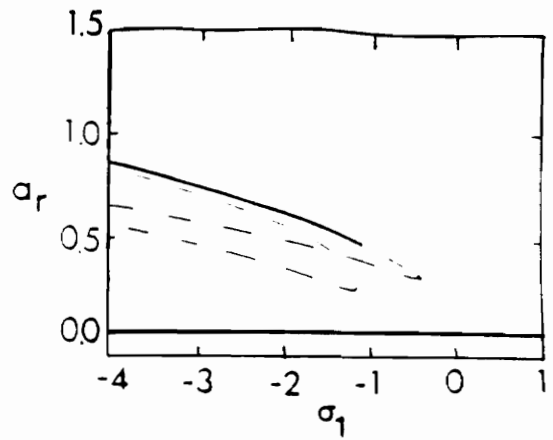
For the cases of nonzero a_r and a_q which are presented as functions of Q in Figure 7, the solution has only one branch. Stable solutions exist in each case for a limited range of Q . One end of the stable portion is located at a point of vertical tangency.

The effect of an internal resonance $\omega_q \simeq 3\omega_r$ on the resonance $\lambda_r + \lambda_q \simeq 2\omega_q$ was illustrated in the previous examples. For a fixed set of parameters, including σ_1 , σ_2 and Q , up to four new steady-state solutions may exist. However, in the cases shown in Figures 5-7, not more than one of the new solutions is stable. Initial conditions determine which solution will occur when more than one stable solution is possible for a set of parameters. Also, the boundary of the stable portion of a solution branch is not always at a point of vertical tangency as it is when the internal resonance is not present or active. Moreover, numerical studies have revealed that at times, when

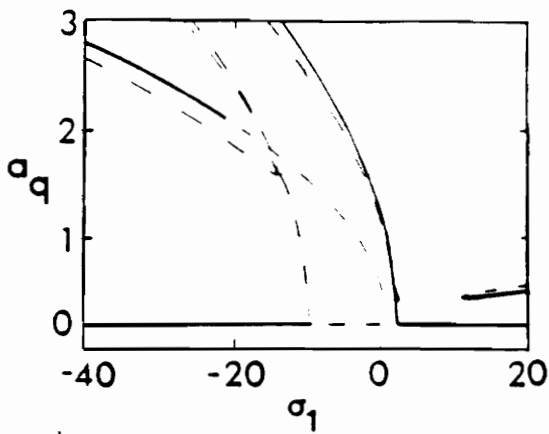
the initial conditions are near one of the unstable branches, the motion never reaches a steady state. Though stable steady states exist for the set of parameters, the modal response amplitudes may oscillate in a limit cycle around the unstable branch.



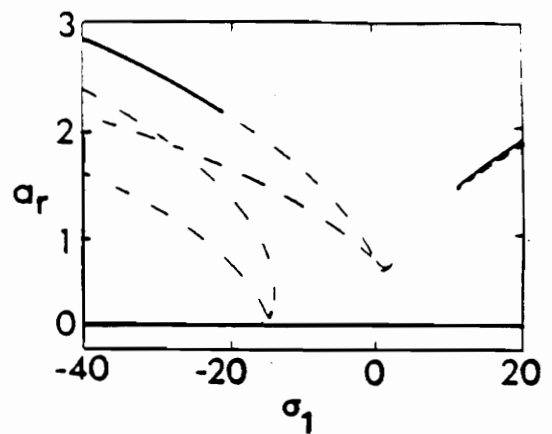
(a)



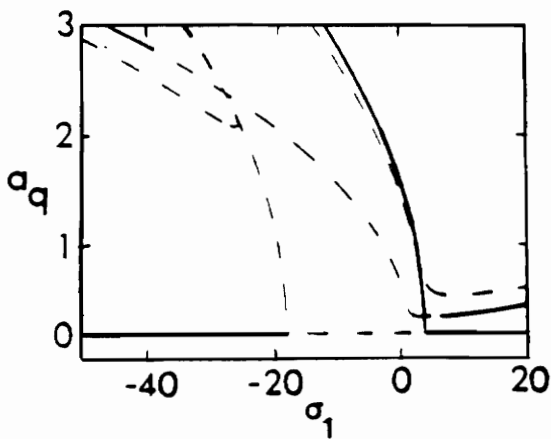
(b)



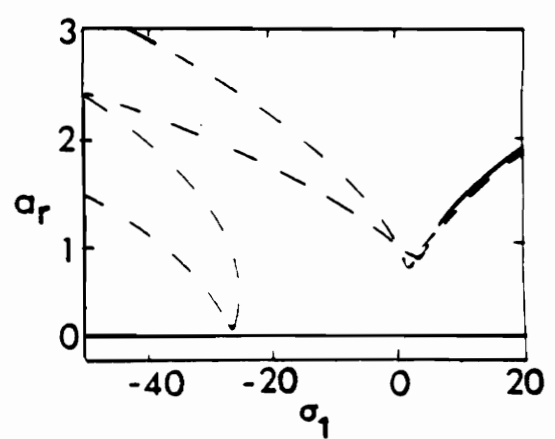
(c)



(d)

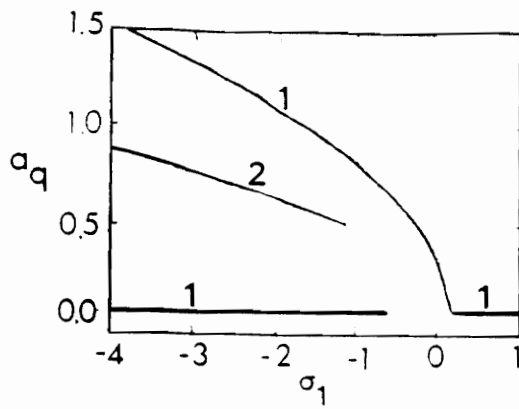


(e)

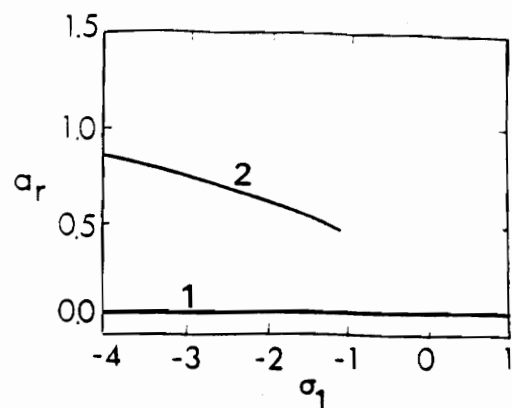


(f)

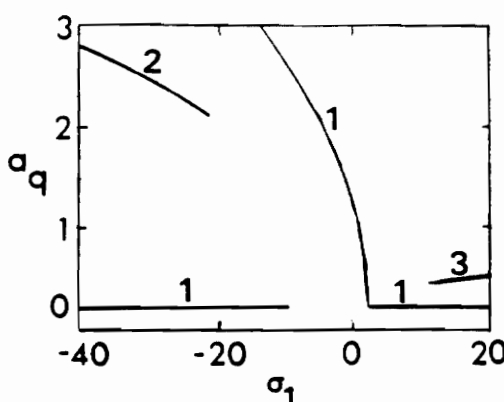
Figure 5. Frequency-response curves: In (a)-(f), $\mu_q = \mu_r = 0.1$, $V_{qr} = W_{rq} = \alpha_{qq} = \alpha_{qr} = \alpha_{rq} = 1$, $\alpha_{rr} = -1$, $\sigma_2 = 0$, $\lambda_2 = 1.5$, $\lambda_1 = 0.5$. In (a) and (b), $Q = 0.388$. In (c) and (d), $Q = 1.494$. In (e) and (f), $Q = 2.028$.



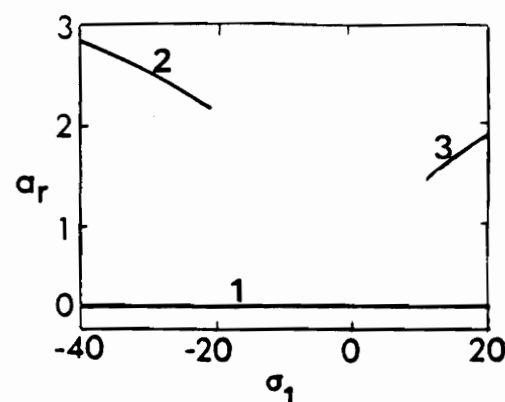
(a)



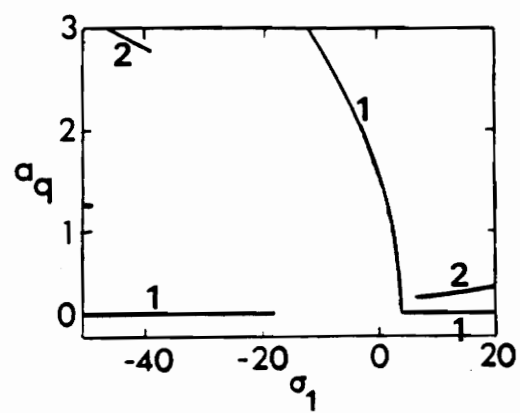
(b)



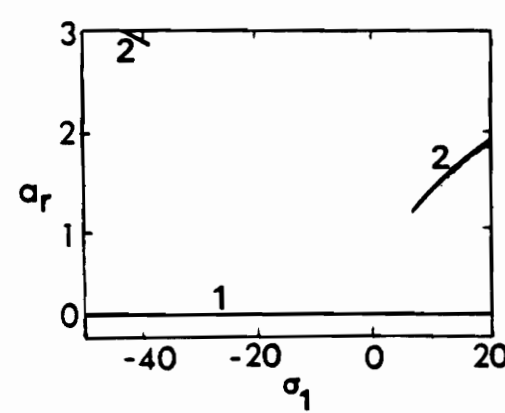
(c)



(d)



(e)



(f)

Figure 6. Frequency-response curves: Repeat of Figure 5 with unstable solutions removed and corresponding solutions marked.

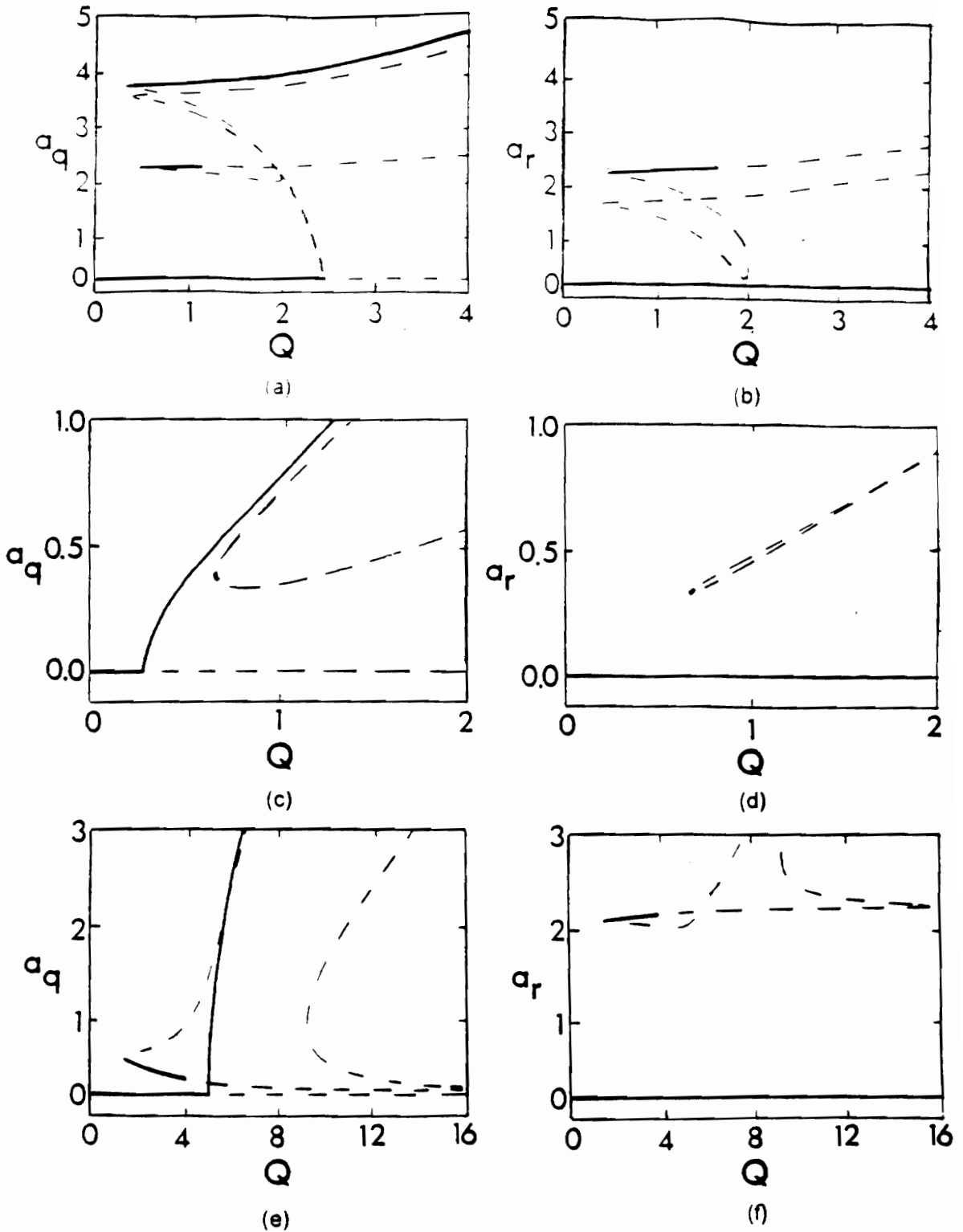


Figure 7. Response amplitudes as functions of excitation amplitude: In (a)-(f), $\mu_q = \mu_r = 0.1$, $V_{qr} = W_{rq} = \alpha_{qq} = \alpha_{qr} = \alpha_{rq} = 1$, $\alpha_{rr} = -1$, $\sigma_2 = 0$, $\lambda_3 = 1.5$, $\lambda_4 = 0.5$. In (a) and (b), $\sigma_1 = -25$. In (c) and (d), $\sigma_1 = 0$. In (e) and (f), $\sigma_1 = 25$.

Chapter 5

The Case When

$$\lambda_s + \lambda_t \simeq 2\omega_q \text{ and } 3\omega_q \simeq \omega_r$$

In this section, we suppose that $\lambda_s + \lambda_t \simeq 2\omega_q$ and $3\omega_q \simeq \omega_r$, and assume no other resonances exist. Detuning parameters, σ_1 and σ_2 , are defined by

$$\lambda_s + \lambda_t = 2\omega_q + \varepsilon^2 \sigma_1 \tag{5.1}$$

$$3\omega_q = \omega_r + \varepsilon^2 \sigma_2. \tag{5.2}$$

As a result, we also have

$$\lambda_s + \lambda_t = \omega_r - \omega_q + \varepsilon^2(\sigma_1 + \sigma_2). \tag{5.3}$$

To eliminate secular terms in the solution for u_{n2} , we use (5.1)-(5.3) and terms 1-4, 15, and 16 of Appendix A, and see that (2.24) becomes

$$\begin{aligned}
& i(D_2 A_n + \mu_n A_n) + e_n A_n - 4A_n \sum_{j=1}^{\infty} \alpha_{jn} A_j \bar{A}_j + \delta_{nq} h_q \bar{A}_q \exp[i(\sigma_1 T_2 + \tau_s + \tau_t)] \\
& - 4\delta_{nq} V_{rq} \bar{A}_q^2 A_r \exp(-i\sigma_2 T_2) - 4\delta_{nr} W_{qr} A_q^3 \exp(i\sigma_2 T_2) \\
& - \delta_{nq} g_{rq} A_r \exp\{-i[(\sigma_1 + \sigma_2)T_2 + \tau_s + \tau_t]\} \\
& - \delta_{nr} p_{qr} A_q \exp\{i[(\sigma_1 + \sigma_2)T_2 + \tau_s + \tau_t]\} = 0
\end{aligned} \tag{5.4}$$

where α_{jn} can be found from (2.25), e_n from (2.26), h_q from (3.3), W_{qr} from (4.4), V_{rq} from (4.5),

$$g_{rq} = \frac{1}{2\omega_q} \sum_{j=1}^{\infty} (R_{j\lambda r}^t Q_{jq1}^s Q_{rj1}^t + R_{j\lambda r}^s Q_{jq1}^t Q_{rj1}^s), \tag{5.5}$$

and

$$p_{qr} = \frac{1}{2\omega_r} \sum_{j=1}^{\infty} (S_{j\lambda q}^t Q_{jr1}^s Q_{qj1}^t + S_{j\lambda q}^s Q_{jr1}^t Q_{qj1}^s). \tag{5.6}$$

Using the form (3.4) in (5.4), we obtain (3.5) and (3.6) for $n \neq q$ or r , and

$$a_q' + \mu_q a_q + h_q a_q \sin \gamma_1 + V_{rq} a_q^2 a_r \sin \gamma_2 + g_{rq} a_r \sin(\gamma_1 + \gamma_2) = 0 \tag{5.7}$$

$$a_q \left(\beta_q' - e_q + \sum_{j=1}^{\infty} \alpha_{jq} a_j^2 - h_q \cos \gamma_1 + V_{rq} a_q a_r \cos \gamma_2 \right) + g_{rq} a_r \cos(\gamma_1 + \gamma_2) = 0 \tag{5.8}$$

$$a_r' + \mu_r a_r - W_{qr} a_q^3 \sin \gamma_2 - p_{qr} a_q \sin(\gamma_1 + \gamma_2) = 0 \tag{5.9}$$

$$a_r \left(\beta_r' - e_r + \sum_{j=1}^{\infty} \alpha_{jr} a_j^2 \right) + W_{qr} a_q^3 \cos \gamma_2 + p_{qr} a_q \cos(\gamma_1 + \gamma_2) = 0 \quad (5.10)$$

for $n = q$ and r where

$$\gamma_1 = \sigma_1 T_2 + \tau_s + \tau_t - 2\beta_q \quad (5.11)$$

$$\gamma_2 = \sigma_2 T_2 + 3\beta_q - \beta_r. \quad (5.12)$$

In the steady state $a_n' = 0$, $\gamma_1' = 0$, and $\gamma_2' = 0$. For $n \neq q$ or r , $a_n = 0$ is the only steady-state solution, and for $n = q$ and r , a_q , a_r , γ_1 , and γ_2 are governed by

$$a_q(\mu_q + h_q \sin \gamma_1 + V_{rq} a_q a_r \sin \gamma_2) + g_{rq} a_r \sin(\gamma_1 + \gamma_2) = 0 \quad (5.13)$$

$$a_q(\zeta_1 - h_q \cos \gamma_1 + V_{rq} a_q a_r \cos \gamma_2) + g_{rq} a_r \cos(\gamma_1 + \gamma_2) = 0 \quad (5.14)$$

$$\mu_r a_r - W_{qr} a_q^3 \sin \gamma_2 - p_{qr} a_q \sin(\gamma_1 + \gamma_2) = 0 \quad (5.15)$$

$$a_r \zeta_2 + W_{qr} a_q^3 \cos \gamma_2 + p_{qr} a_q \cos(\gamma_1 + \gamma_2) = 0 \quad (5.16)$$

where

$$\zeta_1 = \frac{1}{2} \sigma_1 - e_q + \alpha_{qq} a_q^2 + \alpha_{rq} a_r^2 \quad (5.17)$$

$$\zeta_2 = \frac{3}{2} \sigma_1 + \sigma_2 - e_r + \alpha_{qr} a_q^2 + \alpha_{rr} a_r^2. \quad (5.18)$$

We consider the case (3.28), and see that (5.5) and (5.6) give

$$g_{rq} = 0, \quad p_{qr} = 0. \quad (5.19)$$

A trivial solution, $a_r = a_q = 0$, exists. Nontrivial solutions with both $a_q \neq 0$ and $a_r \neq 0$ are also possible, and these solutions are governed by

$$\mu_q + h_q \sin \gamma_1 + V_{rq} a_q a_r \sin \gamma_2 = 0 \quad (5.20)$$

$$\zeta_1 - h_q \cos \gamma_1 + V_{rq} a_q a_r \cos \gamma_2 = 0 \quad (5.21)$$

$$\mu_r a_r - W_{qr} a_q^3 \sin \gamma_2 = 0 \quad (5.22)$$

$$a_r \zeta_2 + W_{qr} a_q^3 \cos \gamma_2 = 0. \quad (5.23)$$

Stability properties of the nontrivial steady-state solutions are determined by substituting (4.19)-(4.22) into (5.7)-(5.10) and using (5.13)-(5.16) to obtain (4.23) with

$$M_{11} = -(\mu_q + h_q \sin \tilde{\gamma}_1 + 2V_{rq} \tilde{a}_q \tilde{a}_r \sin \tilde{\gamma}_2)$$

$$M_{12} = -(V_{rq} \tilde{a}_q^2 \sin \tilde{\gamma}_2)$$

$$M_{13} = -h_q \tilde{a}_q \cos \tilde{\gamma}_1$$

$$M_{14} = -V_{rq} \tilde{a}_q^2 \tilde{a}_r \cos \tilde{\gamma}_2$$

$$M_{21} = 3W_{qr} \tilde{a}_q^2 \sin \tilde{\gamma}_2$$

$$M_{22} = -\mu_r$$

$$M_{23} = 0$$

$$M_{24} = W_{qr} \tilde{a}_q^3 \cos \tilde{\gamma}_2 \quad (5.24)$$

$$M_{31} = 2(2\alpha_{qq}\tilde{a}_q + V_{rq}\tilde{a}_r \cos \tilde{\gamma}_2)$$

$$M_{32} = 2(2\alpha_{rq}\tilde{a}_r + V_{rq}\tilde{a}_q \cos \tilde{\gamma}_2)$$

$$M_{33} = 2h_q \sin \tilde{\gamma}_1$$

$$M_{34} = -2V_{rq}\tilde{a}_q\tilde{a}_r \sin \tilde{\gamma}_2$$

$$M_{41} = -3(2\alpha_{qq}\tilde{a}_q + V_{rq}\tilde{a}_r \cos \tilde{\gamma}_2) + 2\alpha_{qr}\tilde{a}_q + \frac{3W_{qr}\tilde{a}_q^2}{\tilde{a}_r} \cos \tilde{\gamma}_2$$

$$M_{42} = -3(2\alpha_{rq}\tilde{a}_r + V_{rq}\tilde{a}_q \cos \tilde{\gamma}_2) + 3\alpha_{rr}\tilde{a}_r + \frac{3}{2} \frac{\sigma_1 + \sigma_2}{\tilde{a}_r} + \frac{\alpha_{qr}\tilde{a}_q}{\tilde{a}_r}$$

$$M_{43} = -3h_q \sin \tilde{\gamma}_1$$

$$M_{44} = 3V_{rq}\tilde{a}_q\tilde{a}_r \sin \tilde{\gamma}_2 - \frac{W_{qr}\tilde{a}_q^3}{\tilde{a}_r} \sin \tilde{\gamma}_2.$$

Solutions for δa_q , δa_r , $\delta \gamma_1$, and $\delta \gamma_2$ can be written as (4.25)-(4.28). Once again, any λ_j with a positive real part indicates a perturbation which grows as $t \rightarrow \infty$ and an unstable solution. All eigenvalues with real parts less than zero indicate a decaying perturbation and a stable solution.

Using (4.19)-(4.22) in (5.7)-(5.10), taking advantage of (5.13)-(5.16), and letting $\tilde{a}_q = \tilde{a}_r = 0$ results in (4.29) and (4.30) as the equations governing perturbations from the trivial solution. As in the previous two chapters, the stability of the a_q trivial solution changes when $(\mu_q + h_q \sin \tilde{\gamma}_1) = 0$; however, the stable nontrivial solution for a_q which bifurcates from this point no longer corresponds to a stable trivial solution

for a_r . A trivial a_q indicates a trivial a_r , and vice-versa. Hence, when a perturbation from $\tilde{a}_q = 0$ can grow, we say that the solution $(\tilde{a}_q, \tilde{a}_r) = (0, 0)$ is unstable, and both trivial solutions are then represented by dashed lines in the figures. Equivalently, (3.25) with (3.26) is obtained for $n = q$, and (4.33) with (4.34) is obtained for $n = r$ when the alternative procedure is used to determine the stability properties of the trivial solution. As in the previous two chapters, the two methods for determining the stability of the trivial solution agree completely.

Solving (5.22) for a_r results in

$$a_r = \frac{W_{qr} a_q^3 \sin \gamma_2}{\mu_r}. \quad (5.25)$$

Using (5.25) in (5.23) gives a cubic equation governing a_q^2 :

$$(a_q^2)^3 + \frac{\alpha_{qr} \mu_r^2}{\alpha_{rr} W_{qr}^2 \sin^2 \gamma_2} (a_q^2) + \frac{\mu_r^2}{\alpha_{rr} W_{qr}^2 \sin^2 \gamma_2} \left(\frac{3}{2} \sigma_1 + \sigma_2 + \frac{\mu_r \cos \gamma_2}{\sin \gamma_2} \right) = 0. \quad (5.26)$$

Solving (5.20) for $\sin \gamma_1$, (5.21) for $\cos \gamma_1$, and squaring and adding the results gives

$$h_q^2 = (\mu_q + V_{rq} a_q a_r \sin \gamma_2)^2 + (\zeta_1 + V_{rq} a_q a_r \cos \gamma_2)^2. \quad (5.27)$$

Making use of (3.21) and (3.22) in (5.27) and solving for Q^2 yields

$$Q^2 = \frac{-1 \pm \sqrt{1^2 - 4HJ}}{2H} \quad (5.28)$$

where

$$H = k_2^2 - k_1^2, \quad I = -2k_1(V_{rq}a_q a_r \cos \gamma_2 + K)$$

and

(5.29)

$$J = -[\mu_q^2 + V_{rq}a_q a_r(2\mu_q \sin \gamma_2 + V_{rq}a_q a_r + 2K \cos \gamma_2) + K^2].$$

In (5.29),

$$K = \frac{1}{2} \sigma_1 + \alpha_{qq}a_q^2 + \alpha_{rr}a_r^2. \quad (5.30)$$

Attempts to repeat the solution procedure of the previous section for frequency-response curves (fixing Q , incrementing σ_1 , and solving (5.25), (5.26), and (5.28) numerically for the corresponding γ_2) failed due to the nature of the problem. The solutions are very sensitive for γ_2 near 0 and π . For this reason the iterative procedure which attempted to find γ_2 did not converge on all possible solutions. Therefore, an alternative procedure was used, and γ_2 was removed from the problem.

By squaring and adding (5.22) and (5.23), γ_2 is eliminated, and solving the result for σ_1 gives

$$\sigma_1 = \frac{2}{3} \left(-\sigma_2 - \alpha_{qr}a_q^2 - \alpha_{rr}a_r^2 \pm \sqrt{\frac{W_{qr}^2 a_q^6}{a_r^2} - \mu_r^2} \right). \quad (5.31)$$

Solving (5.20) for $\sin \gamma_1$, (5.21) for $\cos \gamma_1$, squaring and adding the results, and using values for $\sin \gamma_2$ and $\cos \gamma_2$ from (5.22) and (5.23) respectively gives

$$-k_2^2 Q^4 + \left(\mu_q + \frac{V_{rq}a_r^2 \mu_r}{W_{qr}a_q^2} \right)^2 + \left(\xi_1 - \frac{\xi_2 V_{rq}a_r^2}{W_{qr}a_q^2} \right)^2 = 0 \quad (5.32)$$

where ξ_1 is defined by (5.17) and ξ_2 by (5.18). Frequency-response curves can now be obtained by fixing Q and σ_2 , varying a_r , substituting (5.31) into (5.32), and solving the resulting equation numerically for a_q .

In Figure 8 the variation of the response amplitudes, a_q and a_r , as functions of a detuning parameter, σ_1 , are shown for the same values of Q as in the preceding section. For the lowest value of Q , shown in Figures 8(a) and (b), two solutions are possible for most negative values of σ_1 ; however, only the upper solution is stable. Small irregularities seen in Figures 8(a) and (b) grow with Q in Figures 8(c)-(f). Once again, no more than two branches of the solutions are present for any given value of σ_1 , and the lower solution is always unstable. The upper solution is no longer always stable, though. Stable solutions exist for σ_1 very negative, and the stability properties alternate for values of σ_1 sufficiently large, ending in a stable region near the bifurcation point.

The variation of the response amplitudes, a_q and a_r , as a function of Q was determined by specifying σ_1 and σ_2 and varying γ_2 from 0 to 2π . For each value of γ_2 , a_q is found from (5.26), a_r from (5.25) and Q from (5.28).

In Figure 9, the behaviors of a_q and a_r with Q are shown. There is a trivial solution, $a_r = a_q = 0$, and nontrivial solutions with both a_q and a_r nonzero. For a given σ_1 and σ_2 , all nontrivial response amplitudes bifurcate from the trivial solution at the same value of Q .

Consider solutions with both a_q and a_r nontrivial. As seen in Figure 9, the solution has only one branch. Stable solutions exist for negative σ_1 and Q sufficiently large, as seen in Figures 9(a) and (b). Figures 9(c) and (d) show that as σ_1 increases, there are two stable regions with an unstable portion in between. Finally, as σ_1 becomes more positive, stable solutions occur for a limited range of Q near the bifurcation point, as shown in Figures 9(e) and (f).

Figure 10 examines the region in Figures 9(c) and (d) where no stable steady-state solutions exist. The variation of a_r with a_q is periodic for the parameters studied, indicating limit-cycle behavior in this region. Limit cycles for values of Q just inside the unstable area of the nontrivial solution are shown in Figures 10(a) and (c), while a limit cycle for a value of Q near the center of the region where no stable steady states exist can be seen in part (b).

The influence of an internal resonance, $\omega_r \simeq 3\omega_q$, on the parametric resonance, $\lambda_s + \lambda_t \simeq 2\omega_q$, has been examined in this chapter. For each case studied, there are no more than two nontrivial solutions possible, and the lower of these solutions is always unstable. In the previous chapter where $\lambda_s + \lambda_t \simeq 2\omega_q$ and $\omega_q \simeq 3\omega_r$, a stable steady state exists for any given set of parameters and the cases shown; however, in the present chapter, there are regions where no stable steady-state solutions exist. In these regions, limit cycle behavior of the response amplitude has been observed in numerical studies. As before, initial conditions determine which response will occur when more than one stable steady state is present for a fixed set of parameters.

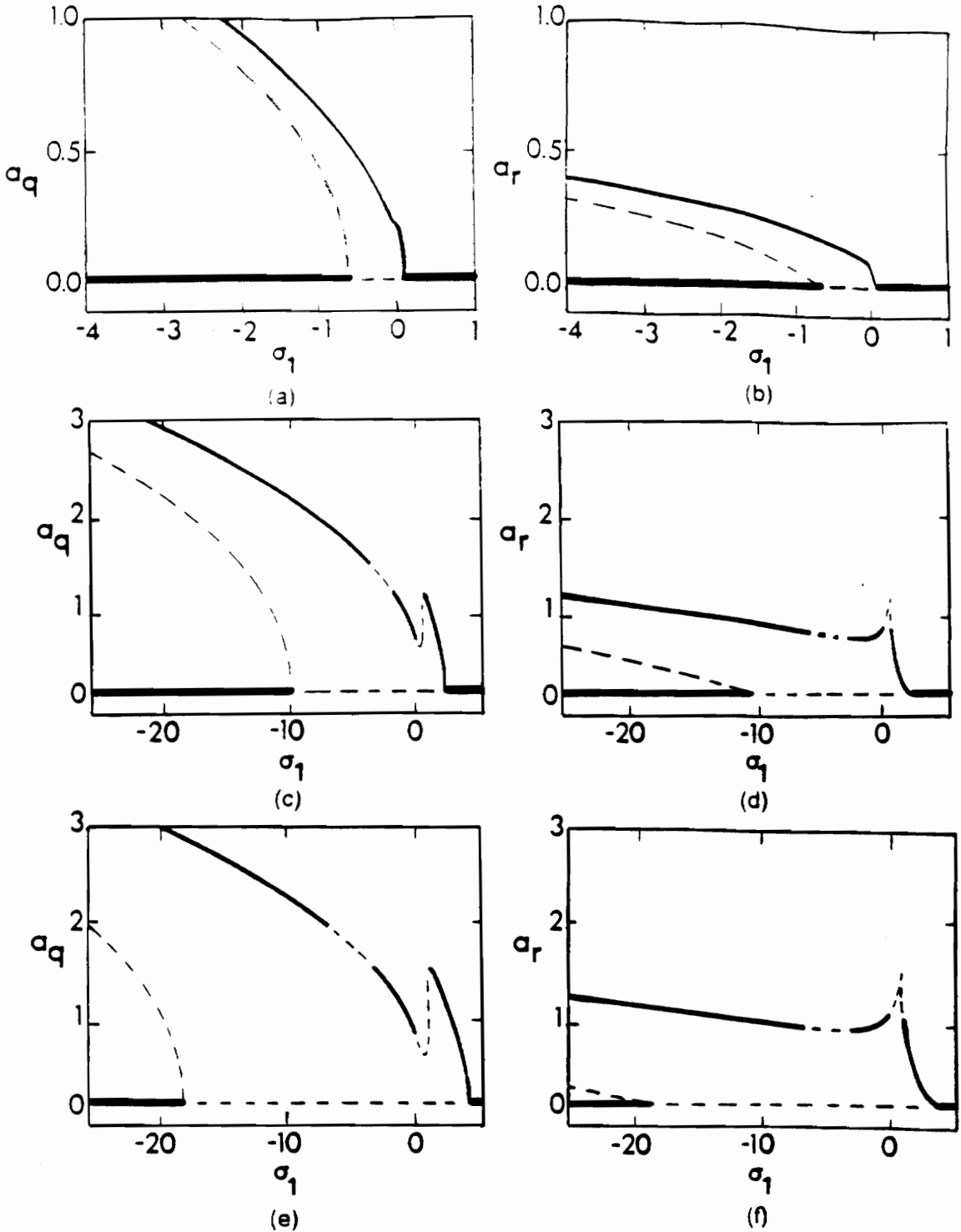


Figure 8. Frequency-response curves: In (a)-(f), $\mu_q = \mu_r = 0.1$, $V_{rq} = W_{qr} = \alpha_{qq} = \alpha_{qr} = \alpha_{rq} = 1$, $\alpha_{rr} = -1$, $\sigma_2 = 0$, $\lambda_s = 1.5$, $\lambda_t = 0.5$. In (a) and (b), $Q = 0.388$. In (c) and (d), $Q = 1.494$. In (e) and (f), $Q = 2.028$.

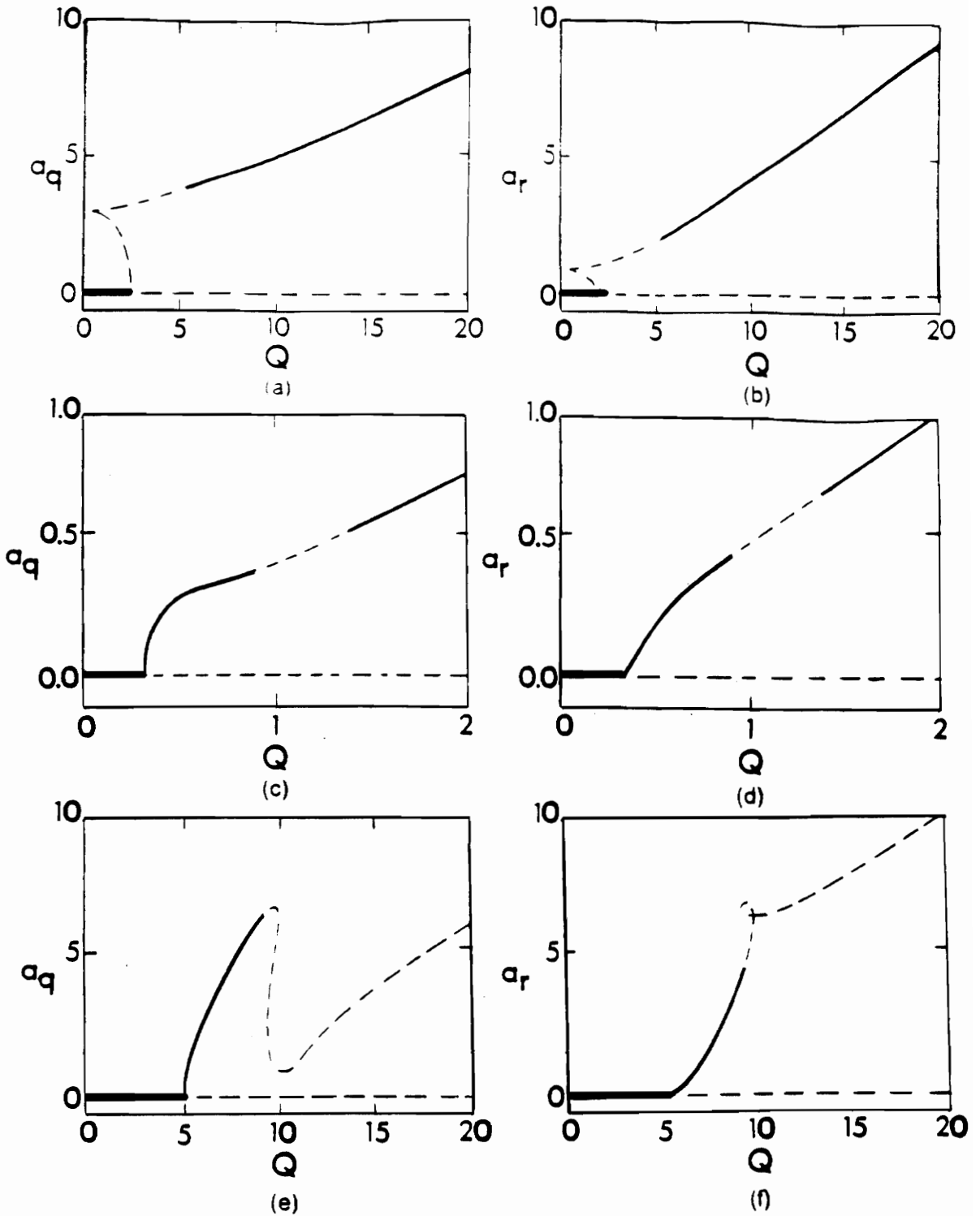


Figure 9. Response amplitudes as functions of excitation amplitude: In (a)-(f), $\mu_q = \mu_r = 0.1$, $V_{rq} = W_{qr} = \alpha_{qq} = \alpha_{qr} = \alpha_{rq} = 1$, $\alpha_{rr} = -1$, $\sigma_2 = 0$, $\lambda_s = 1.5$, $\lambda_t = 0.5$. In (a) and (b), $\sigma_1 = -25$. In (c) and (d), $\sigma_1 = 0$. In (e) and (f), $\sigma_1 = 25$.

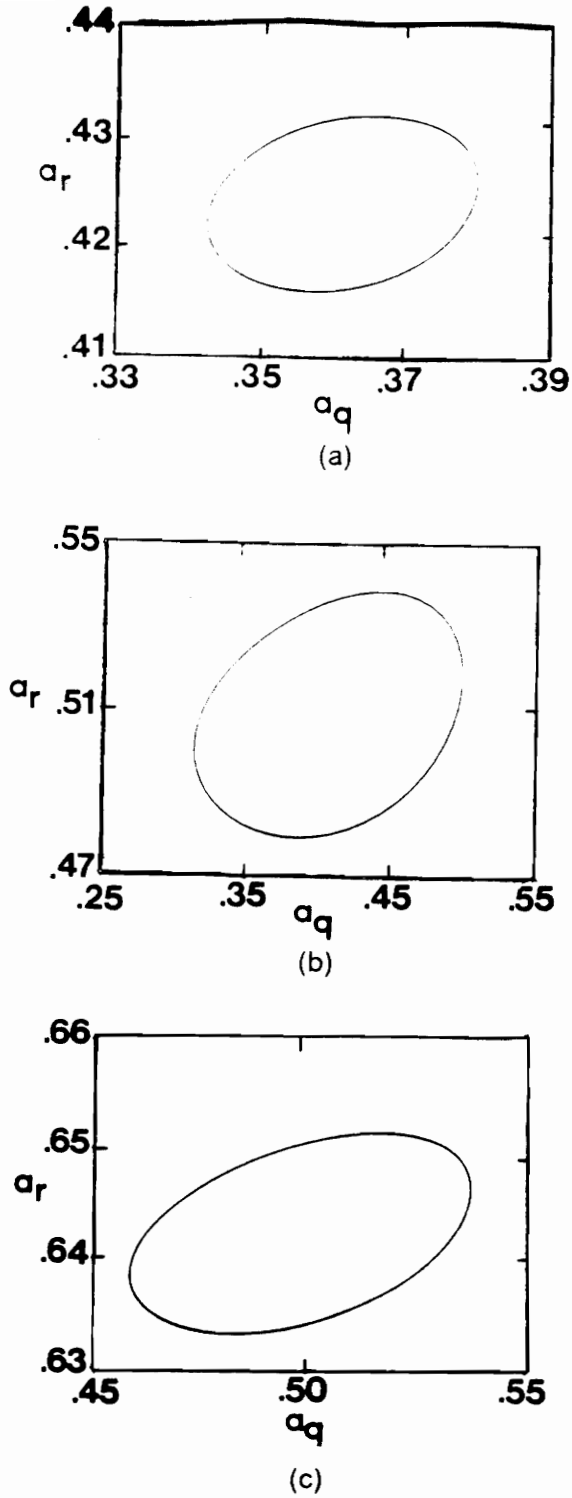


Figure 10. Limit-cycle behavior: Plots of a_r as a function of a_q in a region where no stable steady-state solutions exist. In (a)-(c), $\sigma_1 = 0$. In (a), $Q = 0.904$. In (b), $Q = 1.100$. In (c), $Q = 1.385$.

Bibliography

1. Elmaraghy, R., and Tabarrok, B., "On the Dynamic Stability of an Axially Oscillating Beam," *Journal of the Franklin Institute*, Vol. 300, 1975, pp. 25-39.
2. Mallik, A. K., Kulkarni, S. B., and Ram, K. S., "Parametric Instability of a Periodically Supported Pipe Without and With Vibration Absorbers," *Journal of Applied Mechanics*, Vol. 51, No. 1, March 1984, pp. 159-163.
3. Noah, S. T., and Hopkins, G. R., "Dynamic Stability of Elastically Supported Pipes Conveying Pulsating Fluid," *Journal of Sound and Vibration*, Vol. 71, No. 1, 1980, pp. 103-116.
4. Noah, S. T., and Hopkins, G. R., "A Generalized Hill's Method for the Stability Analysis of Parametrically Excited Dynamic Systems," *Journal of Applied Mechanics*, Vol. 49, No. 1, March 1982, pp. 217-223.
5. Bajaj, A. K., "Interactions Between Self and Parametrically Excited Motions in Articulated Tubes," *Journal of Applied Mechanics*, Vol. 51, No. 2, June 1984, pp. 423-429.
6. Barr, A. D. S., and McWhannell, D. C., "Parametric Instability in Structures Under Support Motion," *Journal of Sound and Vibration*, Vol. 14, No. 4, 1971, pp. 491-509.
7. Schmidt, G., and Tondl, A., *Non-Linear Vibrations*, Akademie-Verlag, Berlin, 1986.
8. Watt, D., and Barr, A. D. S., "Stability Boundary for Pseudo-Random Parametric Excitation of a Linear Oscillator," *Journal of Vibration, Acoustics, Stress, and Reliability in Design*, Vol. 105, July 1983, pp. 326-331.
9. Bogdanoff, J. L., and Citron, S. J., "Experiments With an Inverted Pendulum Subjected to Random Parametric Excitation," *Journal of the Acoustical Society of America*, Vol. 38, No. 8, 1965, pp. 447-452.

10. Nayfeh, A. H., "Response of Two-Degree-of-Freedom Systems to Multifrequency Parametric Excitations," *Journal of Sound and Vibration*, Vol. 88, No. 1, 1983, pp. 1-10.
11. Nayfeh, A. H., and Jebril, A. E. S., "The Response of Two-Degree-of-Freedom Systems with Quadratic and Cubic Non-Linearities to Multifrequency Parametric Excitations," *Journal of Sound and Vibration*, Vol. 115, No. 1, 1987, pp. 83-101.
12. Plaut, R. H., "Parametric Excitation of an Inextensible, Air-Inflated, Cylindrical Membrane," *International Journal of Non-Linear Mechanics*, submitted August 1988.
13. Nayfeh, A. H., and Mook, D. T., *Nonlinear Oscillations*, Wiley-Interscience, New York, 1979.
14. HaQuang, N., "The Response of Multidegree-of-Freedom Systems with Quadratic and Cubic Nonlinearities Subjected to Parametric and External Excitations," Ph.D. Dissertation, Virginia Polytechnic Institute and State University, Blacksburg, Virginia, February, 1986.
15. Mook, D. T., Plaut, R. H., and HaQuang, N., "The Response of Multidegree-of-Freedom Systems With Quadratic and Cubic Nonlinearities, with Application to a Shallow Arch. I: Single-Frequency Excitation," Report VPI-E-83-39, College of Engineering, Virginia Polytechnic Institute and State University, Blacksburg, Virginia, September, 1983.
16. Nayfeh, A. H., *Introduction to Perturbation Techniques*, Wiley-Interscience, New York, 1981.
17. Plaut, R. H., Gentry, J. J., and Mook, D. T., "Nonlinear Oscillations Under Multifrequency Parametric Excitation," *International Journal of Non-Linear Mechanics*, submitted September 1988.

Appendix A

Coefficients and Arguments in Equation (2.20)

y	ϕ_y	ψ_y	v_y	η_y
1	R_{zjk}	$A_j A_k A_l$	$\omega_j + \omega_k + \omega_l$	--
2	R_{zjk}	$A_j A_k \bar{A}_l$	$\omega_j + \omega_k - \omega_l$	--
3	S_{zjk}	$A_j \bar{A}_k A_l$	$\omega_j - \omega_k + \omega_l$	--
4	S_{zjk}	$A_j \bar{A}_k \bar{A}_l$	$\omega_j - \omega_k - \omega_l$	--
5	$R_{l\lambda j}^m$	$A_j A_k$	$\lambda_m + \omega_j + \omega_k$	τ_m
6	$R_{l\lambda j}^m$	$A_j \bar{A}_k$	$\lambda_m + \omega_j - \omega_k$	τ_m
7	$S_{l\lambda j}^m$	$\bar{A}_j A_k$	$\lambda_m - \omega_j + \omega_k$	τ_m
8	$S_{l\lambda j}^m$	$\bar{A}_j \bar{A}_k$	$\lambda_m - \omega_j - \omega_k$	τ_m
9	1	A_j	$\lambda_m + \omega_j$	τ_m
10	1	\bar{A}_j	$\lambda_m - \omega_j$	τ_m
11	R_{ljk}	$A_j A_k$	$\lambda_m + \omega_j + \omega_k$	τ_m
12	S_{ljk}	$A_j \bar{A}_k$	$\lambda_m + \omega_j - \omega_k$	τ_m
13	S_{ljk}	$\bar{A}_j A_k$	$\lambda_m - \omega_j + \omega_k$	τ_m
14	R_{ljk}	$\bar{A}_j \bar{A}_k$	$\lambda_m - \omega_j - \omega_k$	τ_m
15	$R_{k\lambda j}^v$	A_j	$\lambda_m + \lambda_v + \omega_j$	$\tau_m + \tau_v$
16	$S_{k\lambda j}^v$	\bar{A}_j	$\lambda_m + \lambda_v - \omega_j$	$\tau_m + \tau_v$
17	$S_{k\lambda j}^v$	A_j	$\lambda_m - \lambda_v + \omega_j$	$\tau_m - \tau_v$
18	$R_{k\lambda j}^v$	\bar{A}_j	$\lambda_m - \lambda_v - \omega_j$	$\tau_m - \tau_v$

Vita

Jeanette J. "Tina" Gentry was born November 11, 1964 in Nicholas County, West Virginia. After graduating from Charleston High School in Charleston, West Virginia she attended Virginia Polytechnic Institute and State University, where she acquired her Bachelor of Science degree in Engineering Science and Mechanics in 1987. She then began working for a Master's Degree in Engineering Mechanics.

A handwritten signature in black ink, appearing to read "Jeanette J. Gentry". The signature is written in a cursive style with a large, stylized initial 'J'.